

Co-Dynamics of Trypanosomiasis and Cryptosporidiosis

Kazeem Oare Okosun^{1,*}, Mirirai Mukamuri¹ and Oluwole Daniel Makinde²

¹ Department of Mathematics, Vaal University of Technology, Private Bag X021, Vanderbijlpark, 1900, South Africa.

² Faculty of Military Science, Stellenbosch University, Private Bag X2, Saldanha 7395, South Africa

Received: 28 Dec. 2015, Revised: 7 Jul. 2016, Accepted: 9 Jul. 2016

Published online: 1 Nov. 2016

Abstract: In this paper a mathematical model for trypanosomiasis-cryptosporidium co-infection dynamics is investigated to give a theoretical mathematical account of the impact of cryptosporidiosis on trypanosomiasis dynamics. The model steady states are analyzed. The disease-free equilibrium is shown to be locally asymptotically stable when the associated epidemic basic reproduction number for the model is less than unity. The trypanosomiasis only and the cryptosporidiosis only model are each found to exhibit transcritical and backward bifurcation phenomena respectively. While the co-infection model exhibits the possibility of multiple endemic equilibria. From the sensitivity analysis, the trypanosomiasis reproductive number \mathcal{R}_0^{tr} is more sensitive to δ (death due to insecticides) and crypto parameters whenever $\mathcal{R}_0^{cr} > 1$ (crypto reproductive number). While the cryptosporidiosis reproductive number \mathcal{R}_0^{cr} is less sensitive to trypanosomiasis parameters whenever $\mathcal{R}_0^{tr} > 1$ (trypanosomiasis reproductive number). This is an indication that cryptosporidiosis infection may be associated with an increased risk of trypanosomiasis, while trypanosomiasis infection is not associated with an increased risk for cryptosporidiosis. We incorporate time dependent controls, using Pontryagin's Maximum Principle to derive necessary conditions for the optimal control of the disease. Furthermore, the effect of the presence of each infection on the endemicity of the other is investigated and presented numerically.

Keywords: Trypanosomiasis, Cryptosporidiosis, Reproductive Number, Endemic equilibrium

1 Introduction

Tsetse-transmitted African animal trypanosomiasis hinders the establishment of developmental and sustainable agricultural systems in more than 30 countries of sub-Saharan Africa (FAO, 2001). Tsetse-transmitted Trypanosomiasis diseases are caused by protozoa of the genus *Trypanosoma* which affects all domestic animals. Most tsetse transmission is cyclic and begins when blood from a trypanosome-infected animal is ingested by the fly. The trypanosome then loses its surface coat and multiplies in the fly, thereafter it reacquires a surface coat and becomes infective. *T. brucei* spp migrate from the gut to the proventriculus to the pharynx and eventually to the salivary glands; while the cycle for *T. congolense* stops at the hypopharynx, and the salivary glands are not invaded. The entire cycle for *T. vivax* occurs in the proboscis. The animal-infective form in the tsetse salivary gland is referred to as the metacyclic form. The life cycle in the tsetse may be as short as 1 week with *T. vivax* or extend to a few weeks for *T. brucei* spp. Severity of disease varies with species and age of the animal infected and the

species of trypanosome involved. The incubation period is usually 1 week to 4 weeks. The primary clinical symptoms are intermittent fever, anemia, and weight loss. Cattle usually have a chronic course with high mortality, especially if there is poor nutrition or other stress factors. Ruminants may gradually recover if the number of infected tsetse flies is low; however but stress results in relapse [28].

Control measures include eradication of tsetse flies (if possible) and use of prophylactic drugs. Tsetse flies can be partially controlled by frequent spraying and dipping of animals, aerial and ground spraying of insecticides on fly-breeding areas, use of insecticide-impregnated screens and targets, bush clearing, and other methods. The trypanosomes that cause tsetse-transmitted trypanosomiasis (sleeping sickness) in animals, *T. brucei brucei*, closely resemble *T. brucei rhodesiense* and *T. brucei gambiense* from people, which requires that adequate precautions should be taken when working with such isolates [28]. Humans and animals cannot be

* Corresponding author e-mail: kazeemoare@gmail.com

infected through direct contact with each other, so tsetse flies remains the vehicle for the spread of the disease [27].

Cryptosporidiosis on the other hand is a diarrheal disease caused by microscopic parasites, *Cryptosporidium*, that can live in the intestine of humans and animals and is passed in the stool of an infected person or animal. Both the disease and the parasite are commonly known as “Crypto”. The parasite is protected by an outer shell that allows it to survive outside the body for long periods of time and makes it very resistant to chlorine-based disinfectants. During the past 2 decades, Crypto has become recognized as one of the most common causes of waterborne disease (recreational water and drinking water) in humans in the United States. Millions of Crypto germs can be released in a bowel movement from an infected human or animal. Shedding of Crypto in the stool begins when the symptoms begin and can last for weeks after the symptoms (e.g., diarrhea) stop [24]. *Cryptosporidium* may be found in soil, food, water, or surfaces that have been contaminated with the feces from infected humans or animals. Crypto is not spread by contact with blood. Crypto can be spread by:

- Putting something in your mouth or accidentally swallowing something that has come into contact with stools of a person or animal infected with Crypto.
- Swallowing recreational water contaminated with Crypto. Recreational water is water in swimming pools, hot tubs, Jacuzzis, fountains, lakes, rivers, springs, ponds, or streams. Recreational water can be contaminated with sewage or feces from humans or animals.
- Swallowing water or beverages contaminated with stools from infected humans or animals.
- Eating uncooked food contaminated with Crypto. Thoroughly wash with uncontaminated water all vegetables and fruits you plan to eat raw.

Although cryptosporidium infection itself isn't life-threatening, but if an immune system is compromised through diseases such as trypanosomiasis, then a cryptosporidium infection can become life-threatening without proper treatment [29]. *Cryptosporidium* infection can be prevented by practicing good hygiene and avoiding swallowing water from pools, recreational water parks, lakes and streams. Therefore, cryptosporidiosis remains an important global cause of morbidity and mortality, capable of causing periodic epidemic disease.

Hence, a good understanding of the transmission dynamics and ecology of trypanosomiasis-cryptosporidiosis co-infection in emergent epidemic regions can help to improve the control of future epidemics. Mathematical models provide a quantitative and potentially valuable tool for this purpose.

Recently, the authors in [15] presented and analyzed a deterministic model for the co-infection of HIV and malaria in a community. Also, in [19], the authors examined a deterministic model for the co-infection of

tuberculosis and malaria, while in [17,?] the authors proposed a model for Schistosomiasis and HIV/AIDS co-dynamics and a deterministic model for malaria and typhoid co-infection. Also, in [1], the authors presented a mathematical assessment of the effect of traditional beliefs and customs on ebola transmission. In [20], a mathematical model for cholera which include essential components such as hyper-infectious, short-lived bacterial state, a separate class for mild human infections and waning disease immunity was formulated and analyzed. An optimal control analysis of hepatitis C virus with acute and chronic stages was presented in [23]. In [32], a global dynamics of an hepatitis C virus was studied. The authors in Nyabadza et.al [21], presented the implications of HIV treatment on the HIV-malaria coinfection dynamics. A simple mathematical model was presented in [16] to assess whether HIV infection is associated with an increased risk for cholera or not. While the co-infection dynamics of malaria and cholera were studied in [22]. The authors in [33] presented a qualitative analysis of a mathematical model for malaria transmission and its variation. Hargrove et.al. [6], presented a mathematical model for trypanosomiasis transmission to identify treatment coverages required to break transmission when host populations consisted of various proportions of wild and domestic mammals, and reptiles. However, some few studies have been carried out on the formulation and analysis to cryptosporidiosis, trypanosomiasis or co-infection models. In [25], the author presented a general mathematical model of a vector-borne disease involving two vertebrate host species and one insect vector species. A compartmental model of sleeping sickness is described in [13] that takes into account a density-dependence of the vector population which is subjected to a regulating migratory mechanism. Also, a three-parameter ($k(1) - k(3)$) model for age-dependent adult instantaneous mortality rates was constructed using mark-recapture data for the tsetse fly *Glossina morsitans morsitans* Westwood (Diptera: Glossinidae) in [8]. In [9], the authors presented a spatial model of tsetse (*Glossina palpalis* ssp. and *G. pallidipes*) life cycle incorporating four control measures (aerial spraying of nonresidual insecticides, traps and targets, insecticide-treated livestock (ITL) and the sterile insect technique) in order to assess how much of each of various combinations of these control tactics would be necessary to eradicate the population. The model further included density-independent and dependent mortality rates, temperature-dependent mortality, an age-dependent mortality, two mechanisms of dispersal and a component of aggregation.

To the authors' knowledge no work has been done to investigate the trypanosomiasis-cryptosporidiosis co-infection dynamics.

In this paper, an *SIR* (susceptible, infected, recovered) model for trypanosomiasis-cryptosporidiosis co infection is formulated. The paper is then organized as follows: The model description and the underlying assumptions are

presented in Section 2. In Section 3, the mathematical analysis of the model is presented. While in Section 4, the trypanosomiasis only model is analyzed. Section 5 is devoted to the analysis of the cryptosporidiosis only model. In Section 6, the analysis of the co-infection model is presented. The numerical results and discussions are presented in Section 7. The conclusion is presented in Section 8.

2 Mathematical Model

The total population, denoted by N_l , is divided into sub-populations of Susceptible individuals S_l , individuals infected with trypanosomiasis only I_{lt} , individuals infected with cryptosporidiosis only I_{cr} , individuals infected with both trypanosomiasis and cryptosporidiosis C_{lbt} , individuals who recovered from trypanosomiasis only R_{lt} , individuals who recovered from cryptosporidiosis only R_{cr} , individuals who recovered from both trypanosomiasis and cryptosporidiosis R_{lbt} . So that $N_l = S_l + I_{lt} + I_{cr} + C_{lbt} + R_{lt} + R_{cr} + R_{lbt}$.

The vector population is assumed to comprise just two compartments, susceptible (S_p) and infective (I_p), (so that $N_p = S_p + I_p$) and the concentration of microbes population is E_c .

Susceptible individuals are recruited at rate Λ_l ; they either die from natural causes, at a rate μ_c , or get infected at a rate $\xi_m^* = \beta_c + \beta_l I_p$. Where $\beta_c^* = \frac{\nu I_{cr}}{K + I_{cr}} + E_c$, E_c is the microbes population, ν is the contact rate and the microbes concentration is denoted by K . The transmission rate of trypanosomiasis to livestock is β_l . Infected species either die due to disease, at rate ψ_{3c} or/and ψ_{4c} , they respectively recover due to treatments at rates ρ_c , σ_c and γ_l . Recovered individuals may lose their immunity and move to the susceptible class at rates ν_c , ω_l and α_l . It is also assumed that infected individuals do not recover spontaneously.

Susceptible tsetse flies are generated at a rate Λ_v , they may die, from natural causes, at a rate μ_v , or from contact with insecticides treated cattle, at a rate δ . They become infected after a blood meal from any infective individuals, the probability of blood meal from infectious is given by a_c and the probability of an infected fly bite causing infection is equal to c_c . Susceptible tsetse flies thus become infectious at rate $\lambda = a_c c_c (I_{lt} + C_{lbt})$. Infectious tsetse flies are also assume to die, from natural causes, at a rate μ_v , or from contact with insecticides treated cattle, at a rate δ . It is further assume here that tsetse flies are not involve in the spread of cryptosporidiosis. The resulting

system of equations is shown below:

$$\begin{cases} \frac{d}{dt} S_l = \Lambda_l + \nu_c R_{lt} + \alpha_l R_{lbt} + \omega_l R_{cr} - \mu_c S_l - \xi_m^* S_l \\ \frac{d}{dt} I_{lt} = \beta_l^* S_l - \beta_c I_{lt} - (\mu_c + \psi_{3c} + \rho_c) I_{lt} \\ \frac{d}{dt} I_{cr} = \beta_c S_l - \beta_l^* I_{cr} - (\mu_c + \psi_{4c} + \sigma_c) I_{cr} \\ \frac{d}{dt} C_{lbt} = \beta_l^* I_{cr} + \beta_c I_{lt} - (\gamma_c + \mu_c + \psi_{3c} + \psi_{4c}) C_{lbt} \\ \frac{d}{dt} R_{lt} = \rho_c I_{lt} - (\mu_c + \nu_c) R_{lt} + \varepsilon_l (1 - \gamma_l) C_{lbt} \\ \frac{d}{dt} R_{cr} = \sigma_c I_{cr} - (\omega_l + \mu_c) R_{cr} + (1 - \varepsilon_l) (1 - \gamma_l) C_{lbt} \\ \frac{d}{dt} R_{lbt} = \gamma_l C_{lbt} - (\alpha_l + \mu_c) R_{lbt} \\ \frac{d}{dt} S_p = \Lambda_v - \lambda^* S_p - (\mu_v + \delta) S_p \\ \frac{d}{dt} I_p = \lambda^* S_p - (\mu_v + \delta) I_p \\ \frac{d}{dt} E_c = \pi (I_{cr} + \theta C_{lbt}) - \mu_b E_c \end{cases} \tag{1}$$

here

$$\begin{aligned} \beta_c^* &= \frac{\nu I_{cr}}{K + I_{cr}} + \rho E_c & \lambda^* &= c_c a_c (I_{lt} + C_{lbt}) \\ \beta_l^* &= \beta_l I_p, & \xi_m^* &= \beta_c + \beta_l I_p \end{aligned} \tag{2}$$

3 Mathematical analysis of the model

3.1 Positivity and boundedness of solutions

For the transmission model (1) to be epidemiologically meaningful, it is important to prove that all its state variables are non-negative for all time. In other words, solutions of the model system (1) with non-negative initial data will remain non-negative for all time $t > 0$.

Theorem 1. Let the initial data $S_l(0) \geq 0, I_{lt}(0) \geq 0, I_{cr}(0) \geq 0, C_{lbt}(0) \geq 0, R_{lt}(0) \geq 0, R_{cr}(0) \geq 0, R_{lbt}(0) \geq 0, S_p(0) \geq 0, I_p(0) \geq 0, E_c(0) \geq 0$. Then the solutions $(S_l, I_{lt}, I_{cr}, C_{lbt}, R_{lt}, R_{cr}, R_{lbt}, S_p, I_p, E_c)$ of the model (1) are non-negative for all $t > 0$. Furthermore

$$\limsup_{t \rightarrow \infty} N_l(t) \leq 1 \quad \text{and} \quad \limsup_{t \rightarrow \infty} N_p(t) \leq 1$$

with,

$$N_l = S_l + I_{lt} + I_{cr} + C_{lbt} + R_{lt} + R_{cr} + R_{lbt}; \quad \text{and}$$

$$N_p = S_p + I_p; \quad E_c.$$

Proof. Let $t_1 = \sup\{t > 0 : S_l(t) > 0, I_{lt}(t) > 0, I_{cr}(t) > 0, C_{lbt}(t) > 0, R_{lt}(t) > 0, R_{cr}(t) > 0, R_{lbt}(t) > 0, S_p(t) > 0, I_p(t) > 0, E_c(t) > 0\}$. Since $S_l(0) > 0, I_{lt}(0) > 0, I_{cr}(0) > 0, C_{lbt}(0) > 0, R_{lt}(0) > 0, R_{cr}(0) > 0, R_{lbt}(0) > 0, S_p(0) > 0, I_p(0) > 0, E_c(0) > 0$, then, $t_1 > 0$. If $t_1 < \infty$, then $S_l, I_{lt}, I_{cr}, C_{lbt}, R_{lt}, R_{cr}, R_{lbt}, S_p, I_p$ or

E_c is equal to zero at t_1 . It follows from the first equation of the system (1), that

$$\frac{dS_l}{dt} = \Lambda_l + v_c R_{lt} + \alpha_l R_{lbt} + \omega_l R_{cr} - \mu_c S_c - \xi_m^* S_l$$

Thus,

$$\frac{d}{dt} \left\{ S_l(t) \exp \left[(\xi_m^* + \mu_c)t \right] \right\} = (\mu_c + v_c R_{lt} + \alpha_l R_{lbt} + \omega_l R_{cr}) \exp \left[(\xi_m^* - \mu_c)t \right]$$

Hence,

$$S_l(t_1) \exp \left[(\xi_m^* + \mu_c)t \right] - S_l(0) = \int_0^{t_1} (\mu_c + v_c R_{lt} + \alpha_l R_{lbt} + \omega_l R_{cr}) \exp \left[(\xi_m^* - \mu_c)p \right] dp$$

so that,

$$S_l(t_1) = S_l(0) \exp \left[-(\xi_m^* + \mu_c)t_1 \right] + \exp \left[-(\xi_m^* + \mu_c)t_1 \right] \int_0^{t_1} (\mu_c + v_c R_{lt} + \alpha_l R_{lbt} + \omega_l R_{cr}) \exp \left[(\xi_m^* - \mu_c)p \right] dp > 0. \tag{3}$$

It can similarly be shown that $I_{lt} > 0, I_{cr} > 0, C_{lbt} > 0, R_{lt} > 0, R_{cr} > 0, R_{lbt} > 0, S_p > 0, I_p > 0$ and $E_c > 0$ for all $t > 0$. For the second part of the proof, it should be noted that $0 < I_{lt}(t) \leq N_l(t)$ and $0 < I_p(t) \leq N_p(t)$.

Adding the first eight equations and the last three equations of the model (1) gives

$$\begin{aligned} \frac{dN_l(t)}{dt} &= \Lambda_l - \mu_c N_l(t) - \psi_{3c}(I_{lt}(t) + C_{lbt}(t)) - \psi_{4c}(I_{lt}(t) + C_{lbt}(t)), \\ \frac{dN_p(t)}{dt} &= \mu_v - \mu_v N_p(t). \end{aligned} \tag{4}$$

Thus,

$$\begin{aligned} \Lambda_l - \mu_c N_l(t) - \psi_{3c}(I_{lt}(t) + C_{lbt}(t)) - \psi_{4c}(I_{lt}(t) + C_{lbt}(t)) N_l(t) &\leq \frac{dN_l(t)}{dt} \leq \Lambda_l - \mu_c N_l(t), \\ \Lambda_v - (\mu_v + \delta) N_p(t) \leq \frac{dN_p(t)}{dt} &\leq \Lambda_v - \mu_v N_p(t). \end{aligned}$$

Hence, respectively

$$\frac{\Lambda_l}{\mu_c + \psi_{3c} + \psi_{4c}} \leq \liminf_{t \rightarrow \infty} N_l(t) \leq \limsup_{t \rightarrow \infty} N_l(t) \leq \frac{\Lambda_l}{\mu_c},$$

and,

$$\frac{\Lambda_v}{\mu_v} \leq \liminf_{t \rightarrow \infty} N_p(t) \leq \limsup_{t \rightarrow \infty} N_p(t) \leq \frac{\Lambda_v}{\mu_v},$$

as required.

3.2 Invariant regions

Model (1) will be analyzed in a biologically-feasible region as follows. The system (1) is split into individual population $(N_l; \text{with } N_l = S_l + I_{lt} + I_{cr} + C_{lbt} + R_{lt} + R_{cr} + R_{lbt})$ and the vector population $(N_p; \text{with } N_p = S_p + I_p)$. Consider the feasible region

$$\mathcal{D} = \mathcal{D}_l \cup \mathcal{D}_p \cup \mathcal{D}_B \subset \mathbb{R}_+^7 \times \mathbb{R}_+^2 \times \mathbb{R}_+^1$$

with,

$$\mathcal{D}_l = \left\{ (S_l, I_{lt}, I_{cr}, C_{lbt}, R_{lt}, R_{cr}, R_{lbt}) \in \mathbb{R}_+^7 : S_l + I_{lt} + I_{cr} + C_{lbt} + R_{lt} + R_{cr} + R_{lbt} \leq N_l \right\},$$

$$\mathcal{D}_B = \left\{ E_c \in \mathbb{R}_+^1 : E_c \right\}.$$

and

$$\mathcal{D}_p = \left\{ (S_p, I_p) \in \mathbb{R}_+^2 : S_p + I_p \leq N_p \right\}.$$

The following steps are followed to establish the positive invariance of \mathcal{D} (i.e., solutions in \mathcal{D} remain in \mathcal{D} for all $t > 0$). The rate of change of the individual and vector populations is given in equation (4), it follows that

$$\begin{aligned} \frac{dN_l(t)}{dt} &\leq \Lambda_l - \mu_c N_l(t), \\ \frac{dN_p(t)}{dt} &\leq \Lambda_v - \mu_v N_p(t). \end{aligned} \tag{5}$$

A standard comparison theorem [11] can then be used to show that $N_l(t) \leq N_l(0)e^{-\mu_c t} + (1 - e^{-\mu_c t}) \frac{\Lambda_l}{\mu_c}$ and $N_p(t) \leq N_p(0)e^{-\mu_v t} + (1 - e^{-\mu_v t}) \frac{\Lambda_v}{\mu_v}$. In particular, $N_l(t) \leq 1$ and $N_p(t) \leq 1$ if $N_l(0) \leq 1$ and $N_p(0) \leq 1$ respectively. Thus, the region \mathcal{D} is positively-invariant. Hence, it is sufficient to consider the dynamics of the flow generated by (1) in \mathcal{D} . In this region, the model can be considered as been epidemiologically and mathematically well-posed [5]. Thus, every solution of the basic model (1) with initial conditions in \mathcal{D} remains in \mathcal{D} for all $t > 0$. Therefore, the ω -limit sets of the system (1) are contained in \mathcal{D} . This result is summarized below.

Lemma 1. *The region $\mathcal{D} = \mathcal{D}_l \cup \mathcal{D}_p \cup \mathcal{D}_B \subset \mathbb{R}_+^7 \times \mathbb{R}_+^2 \times \mathbb{R}_+^1$ is positively-invariant for the basic model (1) with non-negative initial conditions in \mathbb{R}_+^{11}*

4 Trypanosomiasis only model

Here, the trypanosomiasis only model is considered.

$$\begin{cases} \frac{d}{dt}S_l = \Lambda_l + v_c R_{lt} - \mu_c S_l - \beta_l^* S_l \\ \frac{d}{dt}I_{lt} = \beta_l^* S_l - (\mu_c + \psi_{3c} + \rho_c) I_{lt} \\ \frac{d}{dt}R_{lt} = \rho_c I_{lt} - (\mu_c + v_c) R_{lt} \\ \frac{d}{dt}S_p = \Lambda_v - \lambda^* S_p - (\mu_v + \delta) S_p \\ \frac{d}{dt}I_p = \lambda^* S_p - (\mu_v + \delta) I_p \end{cases} \quad (6)$$

hence,

$$\lambda^* = c_c a_c I_{lt}, \quad \beta_l^* = \beta_l I_p \quad (7)$$

4.1 Stability of the disease-free equilibrium for trypanosomiasis only model

The trypanosomiasis only model (6) has a DFE, obtained by setting the right-hand sides of the equations in the model to zero, given by

$$\begin{aligned} \mathcal{E}_0 &= (S_l^*, I_{lt}^*, R_{lt}^*, S_p^*, I_p^*) \\ &= \left(\frac{\Lambda_l}{\mu_c}, 0, 0, \frac{\Lambda_v}{(\mu_v + \delta)}, 0 \right). \end{aligned} \quad (8)$$

The linear stability of \mathcal{E}_0 can be established using the next generation operator method [31] on the system (6), it then follows that the reproductive number for trypanosomiasis only is given by

$$R_0^{lt} = \sqrt{\frac{a_c c_c \Lambda_l \Lambda_v \beta_l}{\mu_c (\delta + \mu_v)^2 (\mu_c + \rho_c + \psi_{3c})}} \quad (9)$$

Theorem 2. *The DFE of the model (6), given by \mathcal{R}_0^{lt} , is locally asymptotically stable (LAS) if $\mathcal{R}_0^{lt} < 1$, and unstable if $\mathcal{R}_0^{lt} > 1$.*

4.2 Existence of endemic equilibrium

$$\begin{cases} S_l^* = \frac{\Lambda_l + v_c R_{lt}^*}{\mu_c + \beta_l^*} \\ I_{lt}^* = \frac{\beta_l^* S_l^*}{(\mu_c + \psi_{3c} + \rho_c)} \\ R_{lt}^* = \frac{\rho_c I_{lt}^*}{v_c + \mu_c} \\ S_p^* = \frac{\Lambda_v}{\mu_v + \delta + \lambda^*} \\ I_p^* = \frac{\lambda^* S_p^*}{\mu_c + \delta} \end{cases} \quad (10)$$

Hence, the trypanosomiasis endemic equilibrium, satisfies the following polynomial

$$P(I_{lt}^*) = I_{lt}^* \left(G_1 (I_{lt}^*)^2 + G_2 (I_{lt}^*) + G_3 \right) = 0 \quad (11)$$

$$\begin{aligned} G_1 &= (\delta + \mu_v) [\mu_c (\mu_c + \rho_c + v_c) + (\mu_c + v_c) \psi_{3c}] [a_c c_c \Lambda_l (\mu_c + v_c) + M_1], \\ G_2 &= \mu_c (\delta + \mu_v) (\mu_c + v_c) (\mu_c + \rho_c + \psi_{3c}) [a_c c_c \Lambda_l (\mu_c + v_c) \\ &\quad + 2(\delta + \mu_v) [\mu_c (\mu_c + v_c + \rho_c) + (\mu_c + v_c) \psi_{3c}]], \\ G_3 &= \mu_c^2 (\mu_c + v_c)^2 (\mu_c + \rho_c + \psi_{3c})^2 (\delta + \mu_v)^2 (1 - R_0^{lt})^2 \end{aligned} \quad (12)$$

where

$$M_1 = (\delta + \mu_v) (\mu_c (\mu_c + \rho_c + v_c) + (\mu_c + v_c) \psi_{3c})$$

Proposition 1

1. If $R_0^{lt} \geq 1$ then system (6) exhibits a transcritical bifurcation.
2. If $R_0^{lt} \leq 1$ then system (6) has no endemic equilibrium.

Proof.

For $R_0^{lt} > 1$ that $G_3 < 0$. This implies that system (6) has a unique endemic steady state. If $R_0^{lt} \leq 1$, then $G_3 \geq 0$ and since $G_2 \geq 0$, in this case system (6) has no endemic steady states.

5 Cryptosporidiosis only model

The cryptosporidiosis only model is considered here.

$$\begin{cases} \frac{d}{dt}S_l = \Lambda_l + \omega_l R_{cr} - \mu_c S_l - \beta_c S_l \\ \frac{d}{dt}I_{cr} = \beta_c S_l - (\mu_c + \psi_{4c} + \sigma_c) I_{cr} \\ \frac{d}{dt}R_{cr} = \sigma_c I_{cr} - (\omega_l + \mu_c) R_{cr} \\ \frac{d}{dt}E_c = \pi I_{cr} - \mu_b E_c \end{cases} \quad (13)$$

here,

$$\beta_c^* = \frac{v(I_{cr})}{K + I_{cr}} + \rho E_c, \tag{14}$$

5.1 Stability of the disease-free equilibrium for cryptosporidiosis only model

The cryptosporidiosis only model (13) has a DFE, obtained by setting the right-hand sides of the equations in the model to zero, given by

$$\begin{aligned} \mathcal{E}_0 &= (S_l^*, I_{cr}^*, R_{cr}^*, E_c^*) \\ &= \left(\frac{\Lambda_l}{\mu_c}, 0, 0, 0 \right). \end{aligned} \tag{15}$$

The linear stability of \mathcal{E}_0 can be established using the next generation operator method [31] on the system (13), it then follows that the reproductive number of cryptosporidiosis only is given by

$$R_0^{cr} = \frac{v\Lambda_l\sqrt{\mu_b} + \sqrt{(v^2\Lambda_l^2\mu_b + 4K^2\pi\mu_c^2\rho(\mu_c + \sigma_c + \psi_{4c}))}}{2K\mu_c\sqrt{\mu_b}(\mu_c + \sigma_c + \psi_{4c})} \tag{16}$$

Theorem 3. *The DFE of the model (13), given by \mathcal{R}_0^{cr} , is locally asymptotically stable (LAS) if $\mathcal{R}_0^{cr} < 1$, and unstable if $\mathcal{R}_0^{cr} > 1$.*

5.2 Existence of endemic equilibrium

$$\begin{cases} S_l^* = \frac{\Lambda_l + \omega_l R_{cr}^*}{\mu_c + \beta_c^*} \\ R_{cr}^* = \frac{\sigma_c I_{cr}^*}{\omega_c + \mu_c} \\ E_c^* = \frac{\pi I_{cr}^*}{\mu_b} \end{cases} \tag{17}$$

and hence, the cryptosporidiosis endemic equilibrium, satisfies the following polynomial

$$P(I_{cr}^*) = I_{cr}^* \left(F_1(I_{cr}^*)^2 + F_2(I_{cr}^*) + F_3 \right) = 0 \tag{18}$$

$$\begin{aligned} F_1 &= \rho\rho_c(\mu_c(\mu_c + \sigma_c + \psi_{4c}) + (\mu_c + \psi_{4c})\omega_l), \\ F_2 &= \frac{K\mu_b\mu_c(\mu_c + \sigma_c + \psi_{4c})}{v\mu_b + K\rho\rho_c}(R_k - R_0^{cr}), \\ F_3 &= K\mu_b\mu_c(\mu_c + \omega_l)(\mu_c + \sigma_c + \psi_{4c})(1 - R_0^{cr}) \end{aligned} \tag{19}$$

where

$$R_k = \frac{(v\mu_b + K\rho\rho_c)(K\rho\rho_c[\mu_c^2 + (\mu_c + \omega_l)(\sigma_c + \psi_{4c})] + \mu_c\mu_b(v + \mu_c)(\mu_c + \sigma_c + \psi_{4c} + M_2))}{K\mu_b\mu_c(\mu_c + \sigma_c + \psi_{4c})}$$

$$M_2 = \mu_b\omega_l[\mu_c(\mu_c + \sigma_c + v) + (v + \mu_c)\psi_{4c}]$$

Theorem 4. *For $K = 0$, the cryptosporidiosis only model (13) has no endemic equilibrium*

Theorem 5. *For $K > 0$, the cryptosporidiosis only model (13) exhibits*

1. a transcritical bifurcation if $R_k \geq 1$.
2. a backward bifurcation if $R_k < 1$.

Proof.

1. For $R_k \geq 1$ we obtain when $\mathcal{R}_0^{cr} > 1$ that $F_3 < 0$. This implies that the system (13) has a unique endemic steady state. If $\mathcal{R}_0^{cr} \leq 1$, then $F_3 \geq 0$ and $F_2 \geq 0$. In this case system (13) has no endemic steady states.
2. For $R_k < 1$ we discuss the following cases:
 - i. $\mathcal{R}_0^{cr} > 1$, in this case $F_3 < 0$ and system (13) has a unique endemic steady state.
 - ii. $\mathcal{R}_0^{cr} \leq R_k$, in this case both F_2 and F_3 are positive implying that system (13) has no endemic steady states.
 - iii. $\sqrt{R_k} < \mathcal{R}_0^{cr} < 1$, here $F_3 > 0$ and $F_2 < 0$ while the discriminant of (13), $\Delta(\mathcal{R}_0^{cr}) := F_2^2 - 4F_1F_3$, can be either positive or negative. We have $\Delta(1) = F_2^2 > 0$ and $\Delta(R_k) = -4F_1F_3 < 0$, then there exists \mathcal{R}_{0c}^{cr} such that $\Delta(\mathcal{R}_{0c}^{cr}) = 0$, $\Delta(\mathcal{R}_0^{cr}) < 0$ for $R_k < \mathcal{R}_0^{cr} < \mathcal{R}_{0c}^{cr}$ and $\Delta(\mathcal{R}_0^{cr}) > 0$ for $\mathcal{R}_{0c}^{cr} < \mathcal{R}_0^{cr}$. This together with the signs of F_2 and F_3 imply that system (13) has no endemic steady states when $R_k < \mathcal{R}_0^{cr} < \mathcal{R}_{0c}^{cr}$, one endemic steady state when $\mathcal{R}_0^{cr} = \mathcal{R}_{0c}^{cr}$ and two endemic steady states when $\mathcal{R}_{0c}^{cr} < \mathcal{R}_0^{cr} < 1$.

The existence of backward bifurcation is illustrated numerically in Figure (1(a))

6 The co-infection model

6.1 Stability of the disease-free equilibrium (DFE)

The cryptosporidiosis-trypanosomiasis model (1) has a DFE, obtained by setting the right-hand sides of the equations in the model to zero, given by

$$\begin{aligned} \mathcal{E}_0 &= (S_l^*, I_{lt}^*, I_{lb}^*, C_{lbt}^*, R_{lt}^*, R_{lb}^*, R_{lbt}^*, S_p^*, I_p^*, E_c^*) \\ &= \left(\frac{\Lambda_l}{\mu_c}, 0, 0, 0, 0, 0, 0, \frac{\Lambda_v}{(\mu_v + \delta)}, 0, 0 \right). \end{aligned} \tag{20}$$

The linear stability of \mathcal{E}_0 can be established using the next generation operator method [31] on the system (1), it then follows that the co-infection reproductive number is given by

$$R_{0c} = \max\{R_0^t, R_0^c\} \tag{21}$$

Theorem 6. *The DFE of the model (1), given by \mathcal{R}_{0c} , is locally asymptotically stable (LAS) if $\mathcal{R}_{0c} < 1$, and unstable if $\mathcal{R}_{0c} > 1$.*

6.2 Endemic equilibrium (EEE)

Next we calculate the endemic steady states. Solving system (1) at the equilibrium we obtain $I_{cr}^* = 0$ (which corresponds to the DFE) or

$$H_1 I_{cr}^{*4} + H_2 I_{cr}^{*3} + H_3 I_{cr}^{*2} + H_4 I_{cr}^* + H_5 = 0 \tag{22}$$

Remark: The system (1) has a unique endemic equilibrium E^* if $R_{0c} > 1$ and Cases 1-3 (as declared in Table 1) are satisfied. It could have more than one endemic equilibrium if $R_{0c} > 1$ and Case 4 is satisfied; it could have 2 endemic equilibria if $R_{0c} < 1$ and Cases 2-4 are satisfied.

Theorem 7.

The system (1) has a unique endemic equilibrium E^ if $R_{0c} > 1$ and Cases 1-3 and 6 are satisfied; it could have more than one endemic equilibrium if $R_{0c} > 1$ and Cases 4, 5, 7, and 8 are satisfied; it could have 2 or more endemic equilibria if $R_{0c} < 1$ and Cases 2-8 are satisfied.*

Table 1, shows the existence of multiple endemic equilibria when $R_{0c} < 1$. The Table suggests the possibility of backward bifurcation, where the stable DFE coexists with a stable endemic equilibrium, when the reproduction number is less than unity. Thus, the occurrence of a backward bifurcation has important implications for epidemiological control measures, since an epidemic may persist at steady state even if $R_{0c} < 1$.

Table 1: Number of possible positive real roots of $P(I_{cr}^*)$ for $R_{0c} > 1$ and $R_{0c} < 1$

Cases	H_1	H_2	H_3	H_4	H_5	R_{0c}	No of sign change	No of +ve real roots
1	+	+	+	+	+	$R_{0c} < 1$	0	0
	+	+	+	-	-	$R_{0c} > 1$	1	1
2	+	-	-	-	+	$R_{0c} < 1$	2	0, 2
	+	-	-	-	-	$R_{0c} > 1$	1	1
3	+	+	-	-	+	$R_{0c} < 1$	2	0, 2
	+	+	-	-	-	$R_{0c} > 1$	1	1
4	+	-	+	-	+	$R_{0c} < 1$	4	0, 2, 4
	+	-	+	-	-	$R_{0c} > 1$	3	1, 3
5	+	-	-	+	+	$R_{0c} < 1$	2	0, 2
	+	-	-	+	-	$R_{0c} > 1$	3	1, 3
6	+	+	+	-	+	$R_{0c} < 1$	2	0, 2
	+	+	+	-	-	$R_{0c} > 1$	1	1
7	+	+	-	+	+	$R_{0c} < 1$	2	0, 2
	+	+	-	+	-	$R_{0c} > 1$	3	1, 3
8	+	-	+	+	+	$R_{0c} < 1$	2	0, 2
	+	-	+	+	-	$R_{0c} > 1$	3	1, 3

7 Numerical Simulations

In order to illustrate the results of the foregoing analysis, numerical simulations of the co-infection model are carried out, using parameter values given in Table (2). For the purpose of illustration, some parameter values are assumed. Find below in Table (2) the parameter descriptions and values used in the numerical simulation of the co-infection model.

Figure (1) shows the existence of a backward bifurcation phenomena, a situation where the disease free and endemic equilibrium coexists. The implication of this is that the classical epidemiological requirement for disease eradication of cryptosporidiosis with reproduction number less than unity is no longer sufficient. In Figure (2), the bifurcation diagram shows that when $R_0^t < 1$ there is a stable disease free equilibrium and when $R_0^t > 1$, a stable endemic equilibrium exists. This further confirms the analytical results which shows that a stable endemic equilibrium exists when $R_0^t > 1$ and the disease free equilibrium becomes unstable when this condition holds. Figures (3, 4) illustrate the existence of endemic equilibrium. Figure (5, 6) shows that in both host and microbes, cryptosporidiosis infection is lower and faster to reach equilibrium when trypanosomiasis is present. The effect of trypanosomiasis is therefore to reduce cryptosporidiosis incidence. Also (7, 8) show that in both

Table 2: Description of variables and parameters of the co-infection model (1).

Para.	Description	value	Ref
Trypa.			
ψ_{3c}	trypa. related death	0.006 day^{-1}	[6]
β_l	prob. of getting infected	0.62 day^{-1}	[6]
μ_c	Natural death rate in humans	0.00055 day^{-1}	[6]
μ_v	Natural death rate in tsetse flies	0.03	[6]
ν_c	trypa. immunity waning rate	1 day^{-1}	[6]
ω_l	cryptos. immunity waning rate	0.001	assd
α_1	trypa-cryptos immunity waning rate	0.001	assd
B_l	birth rate	22 day^{-1}	[6]
B_v	tsetse flies birth rate	$1,440 \text{ day}^{-1}$	[6]
γ_c	recovery rate of co-infected	0.0000134	assd
σ_c	recovery rate of cryptos infected	0.07 day^{-1}	assd
ρ_c	recovery rate of trypa. infected	0.034 day^{-1}	assd
ε	co-infected recovering from trypa. only	0.0001	assd
Cryptos			
ν	ingestion rate	0.5	[20]
K	Microbes concentration in environment	1000	assd
ψ_{4c}	cryptos related death	0.02407	assd
π	cryptos. infected contrib. to the environment	0.7	assd
θ	modification parameter	1.2	[16]
μ_b	microbes mortality rate	0.033	[20]
β_c	microbes contact rate with individual	0.05	assd

host and vectors, trypanosomiasis infection is lower and faster to reach equilibrium when cryptosporidiosis is present. The effect of cryptosporidiosis is therefore to reduce trypanosomiasis incidence.

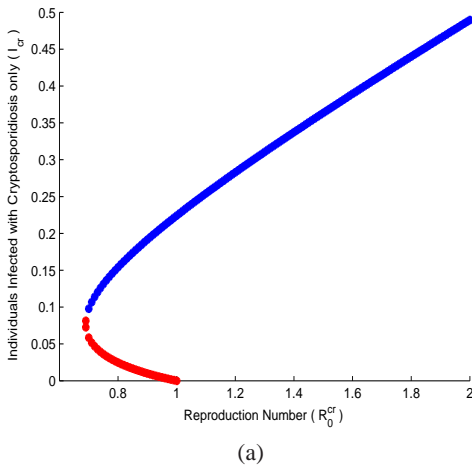


Fig. 1: Simulations of model (1) showing the bifurcation phenomena of cryptosporidiosis and trypanosomiasis.

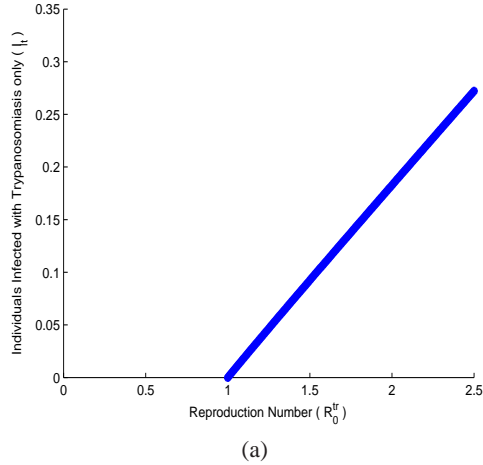


Fig. 2: Simulations of model (1) showing the bifurcation phenomena of cryptosporidiosis and trypanosomiasis.

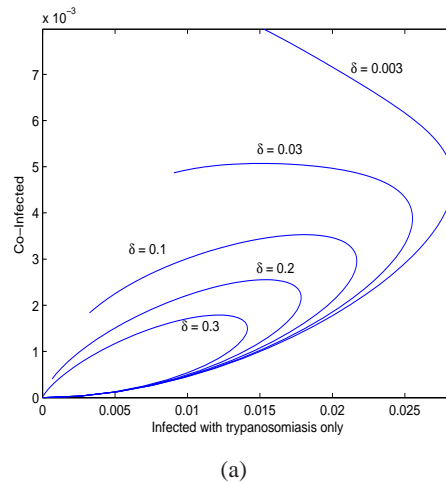


Fig. 3: Simulations of model (1) showing the phase plane of co-infected individuals against individuals infected with trypanosomiasis. The graph shows a phase plane for endemic model with $R_{0c} > 1$. It was obtained by varying the parameter values of δ and μ_c respectively with other parameters fixed as shown in Table (2)

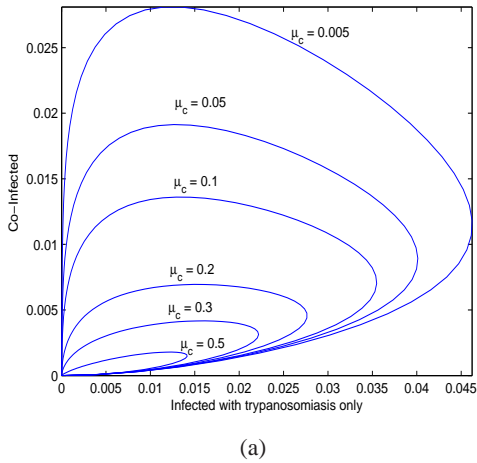


Fig. 4: Simulations of model (1) showing the phase plane of co-infected individuals against individuals infected with trypanosomiasis. The graph shows a phase plane for endemic model with $R_{0c} > 1$. It was obtained by varying the parameter values of δ and μ_c respectively with other parameters fixed as shown in Table (2)

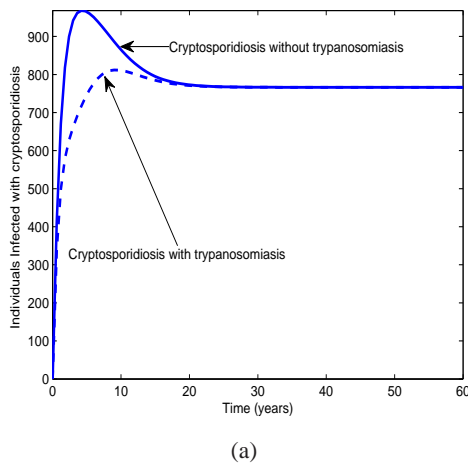


Fig. 5: Simulations of model (1) showing cryptosporidiosis incidence in host and microbes with and without trypanosomiasis infection.

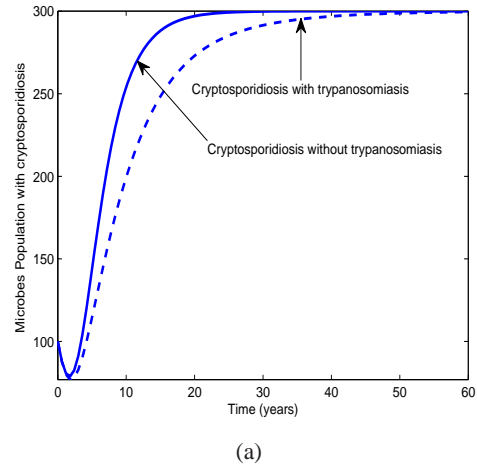


Fig. 6: Simulations of model (1) showing cryptosporidiosis incidence in host and microbes with and without trypanosomiasis infection.

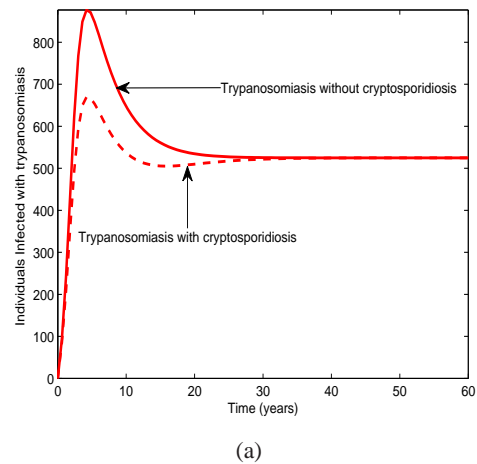
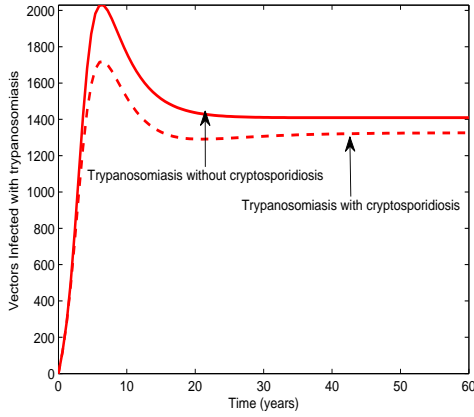
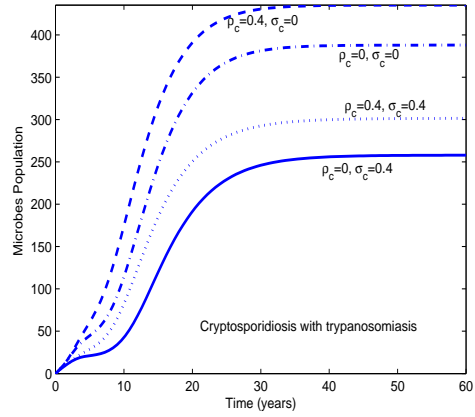


Fig. 7: Simulations of model (1) showing the trypanosomiasis incidence in host and vectors with and without cryptosporidiosis infection is shown. Trypanosomiasis and cryptosporidiosis are simultaneously introduced into a population in the presence and absence of co-infection.



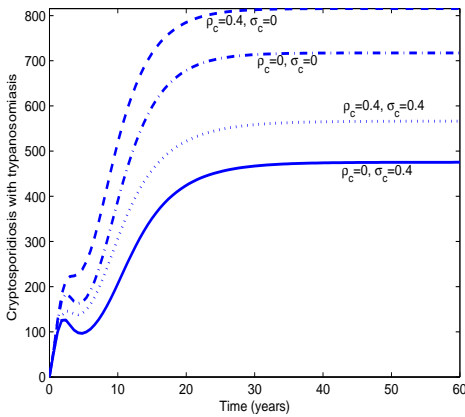
(a)

Fig. 8: Simulations of model (1) showing the trypanosomiasis incidence in host and vectors with and without cryptosporidiosis infection is shown. Trypanosomiasis and cryptosporidiosis are simultaneously introduced into a population in the presence and absence of co-infection.



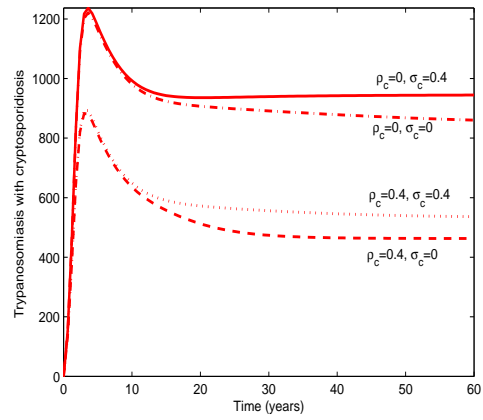
(a)

Fig. 10: Simulations of model (1) showing effect of treatment on cryptosporidiosis in host and microbes with trypanosomiasis infection.



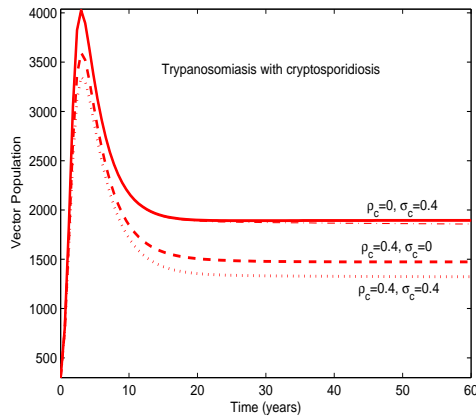
(a)

Fig. 9: Simulations of model (1) showing in effect of treatment on cryptosporidiosis in host and microbes with trypanosomiasis infection.



(a)

Fig. 11: Simulations of model (1) showing effect of treatment on trypanosomiasis in host and vectors with cryptosporidiosis infection is shown. Trypanosomiasis and cryptosporidiosis are simultaneously introduced into a population in the presence and absence of co-infection.



(a)

Fig. 12: Simulations of model (1) showing effect of treatment on trypanosomiasis in host and vectors with cryptosporidiosis infection is shown. Trypanosomiasis and cryptosporidiosis are simultaneously introduced into a population in the presence and absence of co-infection.

8 Sensitivity analysis of the co-infection model

8.1 Sensitivity indices of R_0^{lt} when expressed in terms of R_0^{cr}

We next derive the sensitivity of R_0^{lt} (i.e. expressing it in terms of R_0^{cr}) to each of the 16 different parameters. However, the expression for the sensitivity indices for some of the parameters are complex, so we evaluate the sensitivity indices of these parameters at the baseline parameter values.

The sensitivity index of R_0^{lt} with respect to β_v , for example, is

$$\gamma_{\beta_c}^{R_0^{lt}} \equiv \frac{\partial R_0^{lt}}{\partial \beta_c} \times \frac{\beta_c}{R_0^{lt}} = 0.5. \tag{23}$$

The detailed sensitivity indices of R_0^{lt} resulting from the evaluation to the other parameters of the model are shown in Table 3.

Table 3 shows the parameters, arranged from the most sensitive to the least. For $R_0^{cr} < 1$, the most sensitive parameters are the crypto contributed to the environment, prob. of infection through contact with environment, microbes mortality rate, recovery rate of crypto infected individuals and death due to insecticides ($\pi, \rho, \mu_b, \sigma_c$ and δ , respectively). Since $\gamma_{\beta_c}^{R_0^{lt}} = 0.5$, decreasing (or increasing) the microbes contact with host β_c by 10% decreases (or increases) R_0^{lt} by 5%; similarly, increasing (or decreasing) π by 10%, increases (or decreases) R_0^{lt} by

Table 3: Sensitivity indices of R_0^{lt} expressed in terms of R_0^{cr}

Para.	Descri	Sensitivity if $R_0^{cr} < 1$	Sensitivity if $R_0^{cr} > 1$	
1	π	crypto contributed to enviro.	1.686	0.51
2	ρ	prob. of infection thro enviro.	1.686	0.51
3	μ_b	microbes mortality rate	-1.686	-0.51
4	σ_c	recovery rate from crypto	-0.877	-0.0077
5	δ	death due to insecticides	-0.813	-0.813
6	a_c	prob. of blood meal	0.5	0.5
7	c_c	prob. of a bite causing infection	0.5	0.5
8	K	concentration of microbes	0.5	0.5
9	β_l	prob. of infection thro trypa	0.5	0.5
10	v	ingestion rate	-0.5	-0.5
11	ρ_c	recovery rate from trypa	-0.41	-0.41
12	ψ_{4c}	crypto death related	-0.3	-0.002
13	μ_v	tsetse natural death	-0.188	-0.188
14	ψ_{3c}	trypanosomiasis death related	-0.074	-0.074
15	μ_c	natural death of hosts	-0.014	-0.0068

16.8%. In the same way, increasing (or decreasing) μ_b or δ , decreases (or increases) R_0^{lt} by 16.8% or 8.1% resp. As the following parameters β_l, K and a_c increases/decreases by 10%, the reproduction number of trypanosomiasis, R_0^{lt} , increases/decreases by 5%.

For $R_0^{lt} > 1$, the most sensitive parameters are the death due to insecticides, crypto mortality rate, the prob. of blood meal, the prob. of bites causing infection, crypto contributed to the environment ($\delta, \mu_b, a_c, c_c, \pi$, respectively). Since $\gamma_{\beta_l}^{R_0^{lt}} = 0.5$, increasing (or decreasing) by 10%, increases (or decreases) R_0^{lt} by 5%; similarly, increasing (or decreasing) the π , by 10% increases (or decreases) R_0^{lt} by 5.1%. Also, as parameters K, c_c and a_c increases/decreases by 10%, the reproduction number R_0^{lt} , increases by only 5%.

It is clear that R_0^{lt} is sensitive to changes in R_0^{cr} . That is, the sensitivity of R_0^{lt} to some parameter variations depends on R_0^{cr} ; whenever, $R_0^{cr} < 1$, R_0^{lt} is more sensitive to the model crypto parameters.

8.2 Sensitivity indices of R_0^{cr} when expressed in terms of R_0^{lt}

We next derive the sensitivity of R_0^{cr} (i.e. expressing it in terms of R_0^{lt}) to each of the 16 different parameters. However, the expression for the sensitivity indices for some of the parameters are complex, so we evaluate the sensitivity indices of these parameters at the baseline parameter values.

The sensitivity index of R_0^{cr} with respect to ρ , for example, is

$$\gamma_{\rho}^{R_0^{cr}} \equiv \frac{\partial R_0^{cr}}{\partial \rho} \times \frac{\rho}{R_0^{cr}} = -0.5. \tag{24}$$

The detailed sensitivity indices of R_0^{cr} resulting from the evaluation to the other parameters of the model are shown

in Table 4. Table 4 shows the parameters, arranged from

Table 4: Sensitivity indices of R_0^{cr} expressed in terms of R_0^{lt}

Para.	Description	Sensitivity if $R_0^{lt} < 1$	Sensitivity if $R_0^{lt} > 1$
1	π crypto contributed to environment	-0.5	-0.5
2	μ_b microbes mortality rate	0.5	0.5
3	σ_c recovery rate from crypto	0.37	0.37
4	ψ_{4c} crypto death related	0.127	0.127
5	μ_c natural death of hosts	0.0029	0.0029
6	δ death due to insecticides	-0.00000045	-0.000000018
7	a_c prob. of blood meal	0.00000027	0.000000011
8	c_c prob. of a bite causing infection	0.00000027	0.000000011
9	K concentration of microbes	0.00000027	0.000000011
10	β_c prob. of infection thro crypto	0.00000027	0.000000011
11	β_l prob. of infection thro trypa.	0.00000027	0.000000011
12	v ingestion rate	-0.00000027	-0.000000011
13	ρ_c recovery rate from trypa	-0.00000023	-0.0000000092
14	μ_v tsetse natural death	-0.00000001	-0.0000000041
15	ψ_{3c} trypanosomiasis death related	-0.000000041	-0.0000000016

the most sensitive to the least. For $R_0^{lt} < 1$, the most sensitive parameters are the crypto contributed to the environment, prob. of infection through contact with environment and microbes mortality rate, (π , ρ and μ_b respectively). Since $\gamma_{\rho}^{R_0^{cr}} = -0.5$, decreasing (or increasing) the prob of contact with crypto ρ by 10% increases (or decreases) R_0^{cr} by 5%; similarly, increasing (or decreasing) π by 10%, decreases (or increases) R_0^{cr} by 5%. In the same way, increasing (or decreasing) σ_c or ψ_{4c} , increases (or decreases) R_0^{cr} by 3.7% or 1.3% resp. As the following parameters β_l , K and β_c increases/decreases by 10%, the reproduction number of cryptosporidiosis, R_0^{cr} , increases/decreases by 0.0000027%.

For $R_0^{cr} > 1$, the most sensitive parameters are also the crypto contributed to the environment, prob. of infection through contact with environment and microbes mortality rate, (π , ρ and μ_b respectively). Since $\gamma_{\mu_c}^{R_0^{cr}} = 0.0029$, increasing (or decreasing) μ_c by 10%, increases (or decreases) R_0^{cr} by 0.03%.

It is clear that R_0^{cr} is sensitive to changes in R_0^{lt} . That is, the sensitivity of R_0^{cr} to some parameter variations depends on R_0^{lt} ; whenever, $R_0^{lt} < 1$, R_0^{cr} is less sensitive to the model trypanosomiasis parameters.

9 Optimal control analysis of the model

In this section, we apply Pontryagin’s Maximum Principle to determine the necessary conditions for the optimal control of the co-infection model. We incorporate time dependent controls into the model (3) to determine the optimal strategy for controlling the disease. Hence we

have,

$$\begin{cases} \frac{d}{dt} S_l = \Lambda_l + v_c R_{lt} + \alpha_l R_{lbt} + \omega_l R_{cr} - \mu_c S_l - (1 - u_1) \xi_m^* S_l \\ \frac{d}{dt} I_{lt} = (1 - u_1) \beta_l^* S_l - (1 - u_2) \beta_c^* I_{lt} - (\mu_c + \psi_{3c} + u_3 \rho_c) I_{lt} \\ \frac{d}{dt} I_{cr} = (1 - u_2) \beta_c^* S_l - (1 - u_1) \beta_l^* I_{cr} - (\mu_c + \psi_{4c} + u_4 \sigma_c) I_{cr} \\ \frac{d}{dt} C_{lbt} = (1 - u_1) \beta_l^* I_{cr} + (1 - u_2) \beta_c^* I_{lt} - (u_5 \gamma_l + \mu_c + \psi_{3c} + \psi_{4c}) C_{lbt} \\ \frac{d}{dt} R_{lt} = u_3 \rho_c I_{lt} - (\mu_c + v_c) R_{lt} + \varepsilon_l (1 - u_5 \gamma_l) C_{lbt} \\ \frac{d}{dt} R_{cr} = u_4 \sigma_c I_{cr} - (\omega_l + \mu_c) R_{cr} + (1 - \varepsilon_l) (1 - u_5 \gamma_l) C_{lbt} \\ \frac{d}{dt} R_{lbt} = u_5 \gamma_l C_{lbt} - (\alpha_l + \mu_c) R_{lbt} \\ \frac{d}{dt} S_p = \Lambda_v - (1 - u_1) \lambda^* S_p - (\mu_v + \delta) S_p \\ \frac{d}{dt} I_p = (1 - u_1) \lambda^* S_p - (\mu_v + \delta) I_p \\ \frac{d}{dt} E_c = (1 - u_2) \pi (I_{cr} + \theta C_{lbt}) - \mu_b E_c \end{cases} \quad (25)$$

where,

$$\beta_c^* = \frac{v I_{cr}}{K + I_{cr}} + \rho E_c \quad \lambda^* = c_c a_c (I_{lt} + C_{lbt}) \quad (26)$$

$$\beta_l^* = \beta_l I_p, \quad \xi_m^* = \beta_c^* + \beta_l I_p$$

For this, we consider the objective functional

$$J(u_1, u_2, u_3, u_4, u_5) = \int_0^{t_f} [z_1 I_{lt} + z_2 I_{cr} + z_3 C_{lbt} + z_4 I_v + A u_1^2 + B u_2^2 + C u_3^2 + D u_4^2 + E u_5^2] dt \quad (27)$$

Our control problem involves a situation in which the number of trypanosomiasis infected individuals, cryptosporidiosis infected individuals, co-infected individuals and the cost of applying preventions and treatments controls $u_1(t)$, $u_2(t)$, $u_3(t)$, $u_4(t)$ and $u_5(t)$ are minimized subject to the system (13).

t_f is the final time and the coefficients, $z_1, z_2, z_3, z_4, A, B, C, D, E$ are the balancing cost factors due to scales and importance of the ten parts of the objective function. We seek to find an optimal control, u_1^* , u_2^* , u_3^* , u_4^* and u_5^* , such that

$$J(u_1^*, u_2^*, u_3^*, u_4^*, u_5^*) = \min \{ J(u_1, u_2, u_3, u_4, u_5) | u_1, u_2, u_3, u_4, u_5 \in \mathcal{U} \} \quad (28)$$

where $\mathcal{U} = \{ (u_1, u_2, u_3, u_4, u_5) \text{ such that } u_1, u_2, u_3, u_4, u_5 \text{ are measurable with } 0 \leq u_1 \leq 1, 0 \leq u_2 \leq 1, 0 \leq u_3 \leq g_2, 0 \leq u_4 \leq g_3 \text{ and } 0 \leq u_5 \leq g_4, \text{ for } t \in [0, t_f] \}$ is the control set.

1. The control $u_1(t)$ and $u_2(t)$ represents the efforts on preventing trypanosomiasis and cryptosporidiosis infections respectively.
2. The control on treatment of trypanosomiasis infected individuals $u_3(t)$ satisfies $0 \leq u_3 \leq g_2$, where g_2 is the drug efficacy use for treatment of trypanosomiasis infected individuals.
3. The control on treatment of cryptosporidiosis infected individuals $u_4(t)$ satisfies $0 \leq u_4 \leq g_3$, where g_3 is the drug efficacy use for treatment of cryptosporidiosis infected individuals and,
4. The control efforts on treatment of co-infected individuals $u_5(t)$ satisfies $0 \leq u_5 \leq g_4$, where g_4 is the drug efficacy use for treatment of co-infected individuals.

The necessary conditions that an optimal solution must satisfy come from the Pontryagin et al [?] Maximum Principle. This principle converts (13)-(27) into a problem of minimizing pointwise a Hamiltonian H , with respect to u_1, u_2, u_3, u_4 and u_5 . The adjoint variable associated with the system is represented by M_i , the Hamiltonian is then written as

$$\begin{aligned}
 H = & z_1 I_{It} + z_2 I_{cr} + z_3 C_{lbt} + z_4 I_v + Au_1^2 + Bu_2^2 + Cu_3^2 + Du_4^2 + Eu_5^2 \\
 & + M_{S_I} \{A_I + v_c R_{It} + \alpha_I R_{lbt} + \omega_I R_{cr} - \mu_c S_I - (1 - u_1) \xi_m^* S_I\} \\
 & + M_{I_{It}} \{(1 - u_1) \beta_I^* S_I - (1 - u_2) \beta_c I_{It} - (\mu_c + u_3 \psi_{3c} + \rho_c) I_{It}\} \\
 & + M_{I_{cr}} \{(1 - u_2) \beta_c S_I - (1 - u_1) \beta_I^* I_{cr} - (\mu_c + u_4 \psi_{4c} + \sigma_c) I_{cr}\} \\
 & + M_{C_{lbt}} \{(1 - u_1) \beta_I^* I_{cr} + (1 - u_2) \beta_c I_{It} - (u_5 \gamma_c + \mu_c + \psi_{3c} + \psi_{4c}) C_{lbt}\} \\
 & + M_{R_{It}} \{u_3 \rho_c I_{It} - (\mu_c + v_c) R_{It} + \epsilon_I (1 - u_5 \gamma) C_{lbt}\} \\
 & + M_{R_{cr}} \{u_4 \sigma_c I_{cr} - (\omega_I + \mu_c) R_{cr} + (1 - \epsilon_I) (1 - u_5 \gamma) C_{lbt}\} \\
 & + M_{R_{lbt}} \{u_5 \gamma C_{lbt} - (\alpha_I + \mu_c) R_{lbt}\} \\
 & + M_{S_p} \{A_v - (1 - u_1) \lambda^* S_p - (\mu_v + \delta) S_p\} \\
 & + M_{I_p} \{(1 - u_1) \lambda^* S_p - (\mu_v + \delta) I_p\} \\
 & + M_{E_c} \{(1 - u_2) \pi (I_{cr} + \theta C_{lbt}) - \mu_b E_c\}
 \end{aligned} \tag{29}$$

where $M_{S_I}, M_{I_{It}}, M_{I_{cr}}, M_{C_{lbt}}, M_{R_{It}}, M_{R_{cr}}, M_{R_{lbt}}, M_{S_v}, M_{I_v}$ and M_{E_c} are the adjoint variables or co-state variables. The system of equations is found by taking the appropriate partial derivatives of the Hamiltonian (29) with respect to the associated state variable.

Theorem 8. Given optimal controls $u_1^*, u_2^*, u_3^*, u_4^*, u_5^*$ and solutions

$S_I, I_{It}, I_{cr}, C_{lbt}, R_{It}, R_{cr}, R_{lbt}, S_v, I_v, E_c$ of the corresponding state system (13)- (27) that minimize $J(u_1, u_2, u_3, u_4, u_5)$ over U . Then there exists adjoint variables

$M_{S_I}, M_{I_{It}}, M_{I_{cr}}, M_{C_{lbt}}, M_{R_{It}}, M_{R_{cr}}, M_{R_{lbt}}, M_{E_c}, M_{S_v}, M_{I_v}$ satisfying

$$\frac{-dM_i}{dt} = \frac{\partial H}{\partial i} \tag{30}$$

where $i = S_I, I_{It}, I_{cr}, C_{lbt}, R_{It}, R_{cr}, R_{lbt}, E_c, S_v, I_v$ and with transversality conditions

$$\begin{aligned}
 M_{S_I}(t_f) = M_{I_{It}}(t_f) = M_{I_{cr}}(t_f) = M_{C_{lbt}}(t_f) = M_{R_{It}}(t_f) \\
 = M_{R_{cr}}(t_f) = M_{R_{lbt}}(t_f) = M_{E_c}(t_f) = M_{S_v}(t_f) = M_{I_v}(t_f) = 0
 \end{aligned} \tag{31}$$

and

$$u_1^* = \min \left\{ 1, \max \left(0, \frac{S_I [\beta_c^* + \beta_I I_p] [M_{I_{It}} - M_{S_I}] + \beta_I^* I_{cr} [M_{C_{lbt}} - M_{I_{cr}}] + \lambda^* S_p [M_{I_v} - M_{S_v}]}{2A} \right) \right\}, \tag{32}$$

$$u_2^* = \min \left\{ 1, \max \left(0, \frac{\beta_c^* I_{It} [M_{C_{lbt}} - M_{I_{It}}] + \beta_c^* S_I M_{I_{cr}} - \pi M_{E_c} [I_{cr} + \theta C_{lbt}]}{2B} \right) \right\}, \tag{33}$$

$$u_3^* = \min \left\{ 1, \max \left(0, \frac{\rho_c I_{It} [M_{I_{It}} - M_{R_{It}}]}{2C} \right) \right\}. \tag{34}$$

$$u_4^* = \min \left\{ 1, \max \left(0, \frac{\sigma_c I_{cr} [M_{I_{cr}} - M_{R_{cr}}]}{2D} \right) \right\}. \tag{35}$$

and

$$u_5^* = \min \left\{ 1, \max \left(0, \frac{\gamma C_{lbt} [M_{C_{lbt}} - M_{R_{lbt}}] + \gamma \epsilon_I C_{lbt} M_{R_{It}} + (1 - \epsilon_I) \gamma C_{lbt} M_{R_{cr}}}{2E} \right) \right\}. \tag{36}$$

Proof: Corollary 4.1 of Fleming and Rishel [4] gives the existence of an optimal control due to the convexity of the integrand of J with respect to u_1, u_2, u_3, u_4 and u_5 , a priori boundedness of the state solutions, and the Lipschitz property of the state system with respect to the state variables. The differential equations governing the adjoint variables are obtained by differentiation of the Hamiltonian function, evaluated at the optimal control.

Solving for $u_1^*, u_2^*, u_3^*, u_4^*$ and u_5^* subject to the constraints, the characterization (32-36) can be derived and we have

$$\begin{aligned}
 0 = \frac{\partial H}{\partial u_1} &= 2Au_1 - S_I [\beta_c^* + \beta_I I_p] [M_{I_{It}} - M_{S_I}] - \beta_I^* I_{cr} [M_{C_{lbt}} - M_{I_{cr}}] - \lambda^* S_p [M_{I_v} - M_{S_v}] \\
 0 = \frac{\partial H}{\partial u_2} &= 2Bu_2 - \beta_c^* I_{It} [M_{C_{lbt}} - M_{I_{It}}] - \beta_c^* S_I M_{I_{cr}} + \pi M_{E_c} [I_{cr} + \theta C_{lbt}]
 \end{aligned} \tag{37}$$

$$0 = \frac{\partial H}{\partial u_3} = 2Cu_3 - \rho_c I_{It} [M_{I_{It}} - M_{R_{It}}] \tag{38}$$

$$0 = \frac{\partial H}{\partial u_4} = 2Du_4 - \sigma_c I_{cr} [M_{I_{cr}} - M_{R_{cr}}]$$

$$0 = \frac{\partial H}{\partial u_5} = 2Eu_5 - \gamma C_{lbt} [M_{C_{lbt}} - M_{R_{lbt}}] - \gamma \epsilon_I C_{lbt} M_{R_{It}} - (1 - \epsilon_I) \gamma C_{lbt} M_{R_{cr}} \tag{39}$$

and with transversality conditions

$$M_{S_I}(t_f) = M_{I_{It}}(t_f) = M_{I_{cr}}(t_f) = M_{C_{lbt}} = \dots = M_{I_v}(t_f) = 0, \tag{40}$$

Hence, we obtain (see Lenhart and Workman (2007))

$$\begin{aligned}
 u_1^* &= \frac{S_I [\beta_c^* + \beta_I I_p] [M_{I_{It}} - M_{S_I}] + \beta_I^* I_{cr} [M_{C_{lbt}} - M_{I_{cr}}] + \lambda^* S_p [M_{I_v} - M_{S_v}]}{2A} \\
 u_2^* &= \frac{\beta_c^* I_{It} [M_{C_{lbt}} - M_{I_{It}}] + \beta_c^* S_I M_{I_{cr}} - \pi M_{E_c} [I_{cr} + \theta C_{lbt}]}{2B} \\
 u_3^* &= \frac{\rho_c I_{It} [M_{I_{It}} - M_{R_{It}}]}{2C} \\
 u_4^* &= \frac{\sigma_c I_{cr} [M_{I_{cr}} - M_{R_{cr}}]}{2D} \\
 u_5^* &= \frac{\gamma C_{lbt} [M_{C_{lbt}} - M_{R_{lbt}}] + \gamma \epsilon_I C_{lbt} M_{R_{It}} + (1 - \epsilon_I) \gamma C_{lbt} M_{R_{cr}}}{2E}
 \end{aligned} \tag{41}$$

By standard control arguments involving the bounds on the controls, we conclude

$$u_i^* = \begin{cases} 0 & \text{If } \xi_i^* \leq 0 \\ \xi_i^* & \text{If } 0 < \xi_i^* < 1 \\ 1 & \text{If } \xi_i^* \geq 1 \end{cases}$$

for $i \in 1, 2, 3, 4, 5$ and where

$$\begin{aligned}
 \xi_1^* &= \frac{S_I [\beta_c^* + \beta_I I_p] [M_{I_{It}} - M_{S_I}] + \beta_I^* I_{cr} [M_{C_{lbt}} - M_{I_{cr}}] + \lambda^* S_p [M_{I_v} - M_{S_v}]}{2A} \\
 \xi_2^* &= \frac{\beta_c^* I_{It} [M_{C_{lbt}} - M_{I_{It}}] + \beta_c^* S_I M_{I_{cr}} - \pi M_{E_c} [I_{cr} + \theta C_{lbt}]}{2B}
 \end{aligned}$$

$$\xi_3^* = \frac{\rho_c I_{lt} [M_{I_{lt}} - M_{R_{lt}}]}{2C}$$

$$\xi_4^* = \frac{\sigma_c I_{cr} [M_{I_{cr}} - M_{R_{cr}}]}{2D}$$

$$\xi_5^* = \frac{\gamma_l C_{lbt} [M_{C_{lbt}} - M_{R_{lbt}}] + \gamma_l \varepsilon_l C_{lbt} M_{R_{lt}} + (1 - \varepsilon_l) \gamma_l C_{lbt} M_{R_{cr}}}{2E}$$

Next, we discuss the numerical solutions of the optimality system and the corresponding results of varying the optimal controls u_1, u_2, u_3, u_4 and u_5 , the parameter choices, and the interpretations from various cases.

10 Numerical Simulations

In order to illustrate the results of the foregoing analysis, numerical simulations of the co-infection model are carried out, using parameter values given in Table (2). For the purpose of illustration, some parameter values are assumed. Find below in Table (2) the parameter descriptions and values used in the numerical simulation of the co-infection model.

10.1 Prevention (u_1) and treatment (u_3) of trypanosomiasis only

The trypanosomiasis prevention control u_1 and the trypanosomiasis treatment control u_3 are used to optimize the objective function J while we set the other controls (u_2, u_4 and u_5) relating to cryptosporidiosis to zero. We observed in Figure 13 a significant difference in the number of trypanosomiasis infected humans I_{lt} in the controlled cases compare to the cases without control. The positive effect of this strategy on I_v is shown in Figure 14, where the number of infected vector I_v cases is seen to be significantly controlled. The result in the depicted Figure 16 clearly suggest that this strategy is not very efficient and effective in the control of the number of cryptosporidiosis infected humans I_{cr} and similarly, impact of the cryptosporidiosis controlled cases resulted in the lower microbes population in the environment E_c as shown in Figure 17. While the population of the co-infected humans C_{lbt} shown in Figure 15 show significant difference between the cases without control and the controlled cases. The control profile revealed that the control on prevention u_1 on trypanosomiasis should be maintained at maximum for 15 days before gradually decreasing to zero, while the control on treatment of trypanosomiasis u_3 would only require control efforts of 7% 18.

10.2 Prevention (u_2) and treatment (u_4) of cryptosporidiosis only

The cryptosporidiosis prevention control u_2 and the cryptosporidiosis treatment control u_4 are used to

optimize the objective function J while we set the other controls (u_1, u_3 and u_5) relating to trypanosomiasis to zero. We observed in Figure 19 a continuous rise in the number of trypanosomiasis infected humans I_{lt} cases. This may be connected to the absence of interventions against trypanosomiasis in this strategy. The negative effect of this strategy is also shown in Figure 22, where the number of infected vector I_v cases is seen to be on the increase after 50 days. The result in the depicted Figure 20 clearly suggest that this strategy is very efficient and effective in the control of the number of cryptosporidiosis infected humans I_{cr} and similarly, the positive impact of the cryptosporidiosis controlled cases resulted in the significant control of the Microbes population in the environment E_c as shown in Figure 23. While the population of the co-infected humans C_{lbt} shown in Figure 21 show significant difference between the cases without control and the controlled cases. The control profile revealed that the control on treatment u_4 on cryptosporidiosis should be at maximum till the end of the intervention, while the control on prevention u_2 rises from 15% up to 55% before gradually decreasing to zero at the end of intervention 24.

10.3 Trypanosomiasis and cryptosporidiosis prevention (u_1 and u_2) only

The trypanosomiasis and cryptosporidiosis prevention controls u_1 and the control u_2 are used to optimize the objective function J while we set the other controls (u_3, u_4 and u_5) to zero. That is, preventions only mechanisms are optimized without treatments. We observed in Figure 25 that the number of trypanosomiasis infected humans I_{lt} was significantly controlled before it start rising again at the final time. This may be connected to the fact that treatment of infected individuals is neglected and as a result the disease persists in the community. This effect is also observed in Figure 28 in the control of number of infected vectors I_v . While in Figure 26 the impact of this strategy in controlling the cryptosporidiosis infected individuals I_{cr} yielded positive results because the prevention strategy worked effectively in the control of cryptosporidiosis infected individuals. The effect of this strategy also impact positively on other population classes as shown clearly in Figure 27, 29. This strategy suggest that optimal preventive strategies against trypanosomiasis and cryptosporidiosis in a community while adequate treatment regime is not put in place at the same time would not be an effective approach to controlling co-infection at the final time. The control profile revealed that the control on prevention u_2 on cryptosporidiosis rises to maximum of 90% before decreasing gradually to zero at the end final time, while the control on prevention u_1 rises to 30% before gradually decreasing to zero at the end of intervention 30.

10.4 Trypanosomiasis and cryptosporidiosis treatment (u_3 and u_4) only

The trypanosomiasis and cryptosporidiosis treatment controls u_3 and u_4 are used to optimize the objective function J while we set the other interventions, that is the preventive measures (u_1, u_2 and u_5) to zero. That is, only the treatment mechanisms are optimized without preventions. We observed in Figure 31 that the number of trypanosomiasis infected humans I_{It} was significantly controlled before it start rising again at the final time. This may be connected to the fact that preventions are neglected and as a result the disease persists in the community. This effect is also observed in Figure 34 in the control of number of infected vectors I_v . While in Figure 32 the impact of this strategy in controlling the cryptosporidiosis infected individuals I_{cr} yielded positive results because the treatment strategy worked effectively in the control of both cryptosporidiosis and trypanosomiasis individuals. The effect of this strategy also impact positively on other population classes as shown clearly in Figure 33, 35. This strategy suggest that optimal treatment strategies against trypanosomiasis and cryptosporidiosis in a community while adequate preventive regime is not put in place at the same time would also be an effective approach to controlling co-infection. The control profile revealed that the control on treatment u_4 on cryptosporidiosis should be at maximum till the end of the intervention, while the control on treatment u_3 rises 30% before gradually decreasing to zero at the end of intervention 36.

10.5 Trypanosomiasis and cryptosporidiosis preventions with treatment (u_1, u_2, u_3, u_4, u_5)

In this strategy all the control mechanism (u_1, u_2, u_3, u_4, u_5) are used to optimize the objective function J . That is, both the preventions and treatments of trypanosomiasis and cryptosporidiosis are optimized. We observed in Figure 37 that the number of trypanosomiasis infected humans I_{It} is effectively controlled. The impact of this strategy is also shown in Figure 40, where the number of infected vectors I_v is significantly reduced to zero at the end of the intervention period. The result shown in Figure 38 clearly suggest that this strategy is also very efficient and effective in controlling the number of cryptosporidiosis infected humans I_{cr} and leading also to effective control of the Microbes population E_c as shown in Figure 41. The population of the trypanosomiasis-cryptosporidiosis co-infected humans C_{lbt} shown in Figure 39 show significant difference between the cases without control and the controlled cases. This strategy suggests that optimal prevention and treatment regime against both trypanosomiasis and cryptosporidiosis in a community would be a very effective approach to effectively control both diseases at

the final intervention time. The control profile revealed that the control on cryptosporidiosis treatment u_4 should be at maximum till the end of the intervention, while prevention control u_2 on cryptosporidiosis rises to 50% before gradually decreasing to zero at the end of intervention. Also, this strategy suggests that little control efforts would be required on trypanosomiasis for both diseases to be effectively controlled 42.

11 Concluding remarks

In this paper, we formulated and analysed a deterministic model for the transmission of trypanosomiasis and cryptosporidiosis co-infection that includes use of preventions, treatments of infectives and also performed optimal control analysis of the model. The model was rigorously analysed to gain insights into its qualitative dynamics. We obtained the following results:

1. The trypanosomiasis only model has a locally-stable disease free equilibrium whenever the associated reproduction number is less than unity. Also, the model has a unique endemic equilibrium whenever $\mathcal{R}_0^{It} > 1$.
2. The cryptosporidiosis model has a locally-stable disease free equilibrium whenever the associated reproduction number is less than unity and exhibits the phenomenon of backward bifurcation, which suggests a case where stable disease-free equilibrium co-exists with a stable endemic equilibrium whenever the basic reproductive number is less than unity.
3. The co-infection model has a locally-stable disease free equilibrium whenever the associated reproduction number is less than unity.
4. From the sensitivity analysis, the trypanosomiasis reproductive number \mathcal{R}_0^{It} is more sensitive to δ (death due to insecticides) and crypto parameters whenever $\mathcal{R}_0^{cr} > 1$ (crypto reproductive number). While the cryptosporidiosis reproductive number \mathcal{R}_0^{cr} is less sensitive to trypanosomiasis parameters whenever $\mathcal{R}_0^{It} > 1$ (trypanosomiasis reproductive number). This is an indication that crypto infection may be associated with an increased risk of trypanosomiasis, while trypanosomiasis infection is not associated with an increased risk for crypto.
5. Focusing only on trypanosomiasis intervention strategies (optimal preventions and treatments) while cryptosporidiosis is not under control would lead to effective control of co-infection at the end of the intervention. As clearly shown in Figure 13- 17, where the number of cryptosporidiosis infected individuals and microbes are lower under control compared to cases without control. This is an indication that cryptosporidiosis infection may be associated with an increased risk of trypanosomiasis.
6. That optimal efforts on cryptosporidiosis intervention strategies (optimal preventions and treatments) while

trypanosomiasis is not under control would only result in effective control of cryptosporidiosis only while trypanosomiasis still persist. This is shown in Figure 19-23, where the number of cryptosporidiosis infected individuals are effectively controlled at the final time. This suggests that trypanosomiasis infection is not associated with an increased risk for cryptosporidiosis.

7. Whenever there is co-existence of trypanosomiasis and cryptosporidiosis in the community, our model suggests the incorporation of cryptosporidiosis control measures with the trypanosomiasis intervention strategies for effective trypanosomiasis control.

8. However, the cost may be unbearable to farmers in areas of extreme poverty, most especially the rural poor and some disadvantaged urban populations to combine therapies, it is suggested that policy markers or Government should provide necessary support in this regard.

Acknowledgement

The authors are grateful to the anonymous referee for a careful checking of the details and for helpful comments that improved this paper.

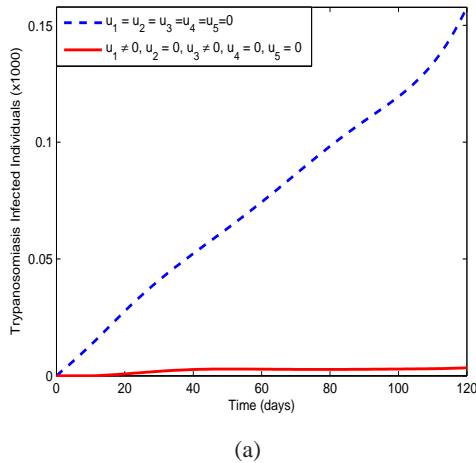


Fig. 13: Simulations of the trypanosomiasis-cryptosporidiosis model showing the effect of trypanosomiasis prevention and treatment only on transmission

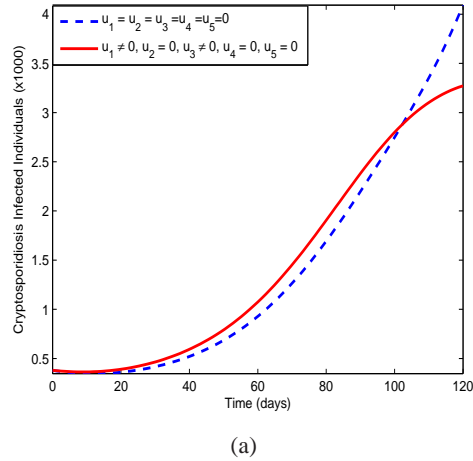


Fig. 14: Simulations of the trypanosomiasis-cryptosporidiosis model showing the effect of trypanosomiasis prevention and treatment only on transmission

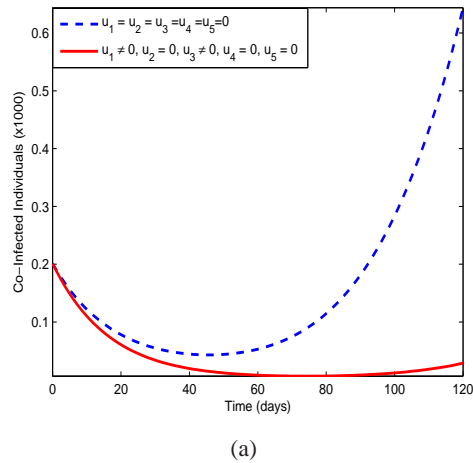
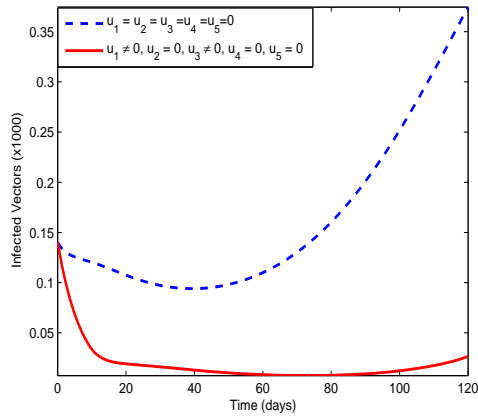
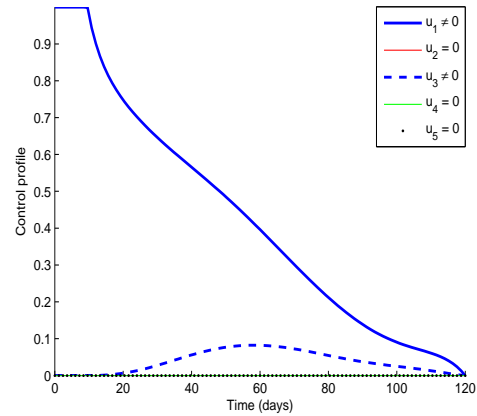


Fig. 15: Simulations of the trypanosomiasis-cryptosporidiosis model showing the effect of trypanosomiasis prevention and treatment only on transmission



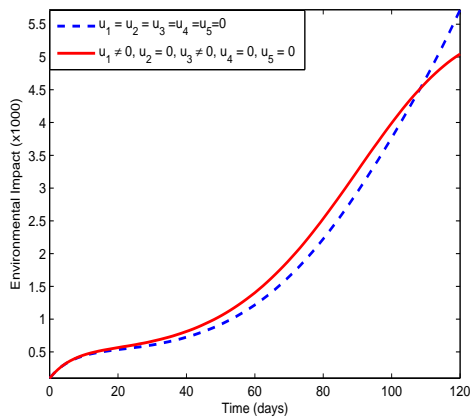
(a)

Fig. 16: Simulations of the trypanosomiasis-cryptosporidiosis model showing the effect of trypanosomiasis prevention and treatment only on transmission



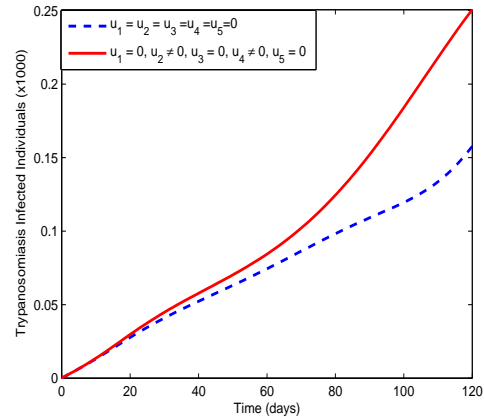
(a)

Fig. 18: Simulations of the trypanosomiasis-cryptosporidiosis model showing the effect of trypanosomiasis prevention and treatment only on transmission



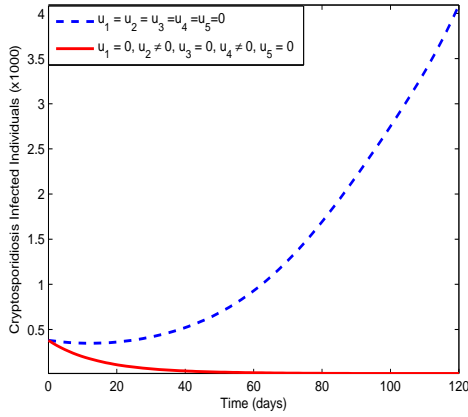
(a)

Fig. 17: Simulations of the trypanosomiasis-cryptosporidiosis model showing the effect of trypanosomiasis prevention and treatment only on transmission

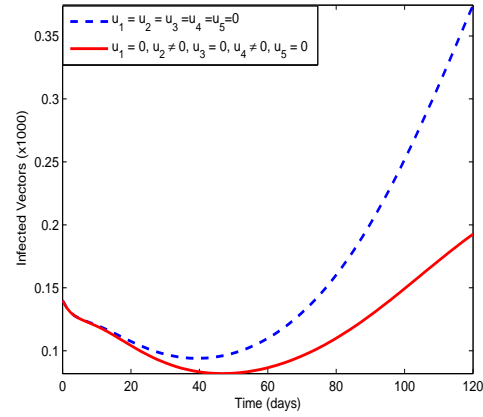


(a)

Fig. 19: Simulations of the trypanosomiasis-cryptosporidiosis model showing the effect of cryptosporidiosis prevention and treatment only on transmission



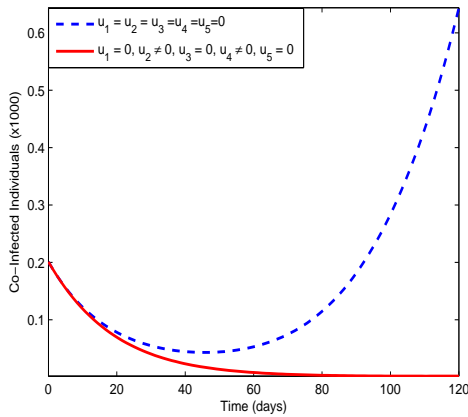
(a)



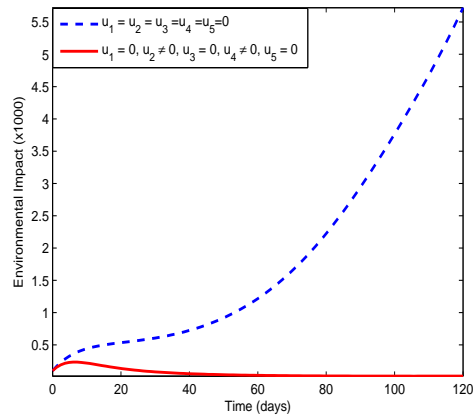
(a)

Fig. 20: Simulations of the trypanosomiasis-cryptosporidiosis model showing the effect of cryptosporidiosis prevention and treatment only on transmission

Fig. 22: Simulations of the trypanosomiasis-cryptosporidiosis model showing the effect of cryptosporidiosis prevention and treatment only on transmission



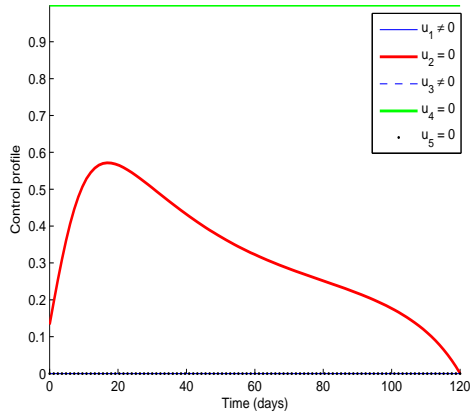
(a)



(a)

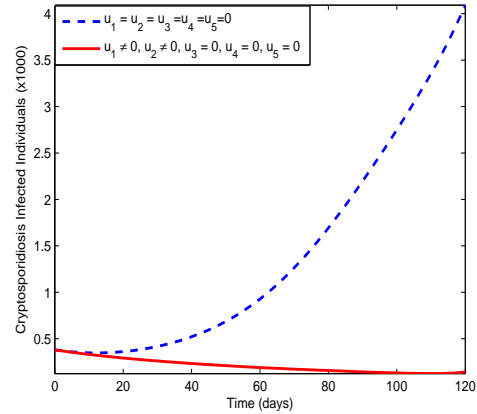
Fig. 21: Simulations of the trypanosomiasis-cryptosporidiosis model showing the effect of cryptosporidiosis prevention and treatment only on transmission

Fig. 23: Simulations of the trypanosomiasis-cryptosporidiosis model showing the effect of cryptosporidiosis prevention and treatment only on transmission



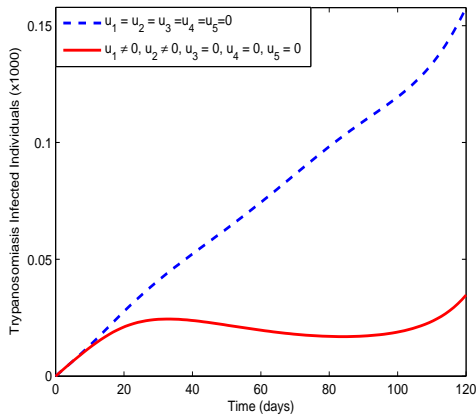
(a)

Fig. 24: Simulations of the trypanosomiasis-cryptosporidiosis model showing the effect of cryptosporidiosis prevention and treatment only on transmission



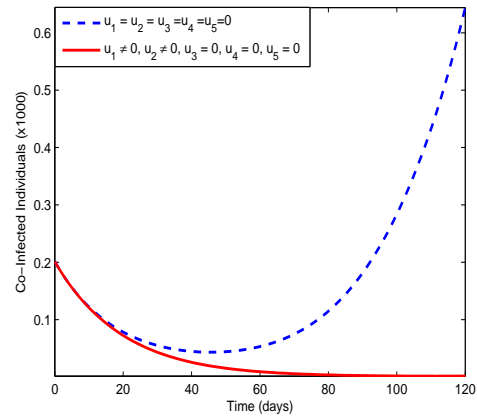
(a)

Fig. 26: Simulations of the trypanosomiasis-cryptosporidiosis model showing the effect of trypanosomiasis and cryptosporidiosis prevention only on transmission



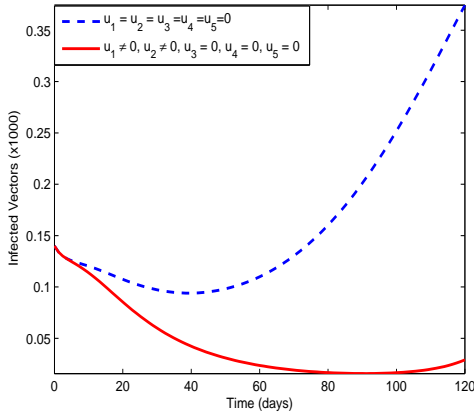
(a)

Fig. 25: Simulations of the trypanosomiasis-cryptosporidiosis model showing the effect of trypanosomiasis and cryptosporidiosis prevention only on transmission



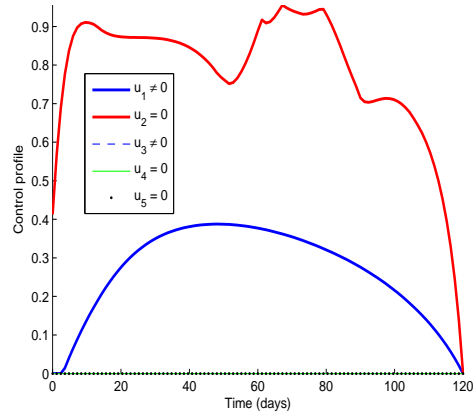
(a)

Fig. 27: Simulations of the trypanosomiasis-cryptosporidiosis model showing the effect of trypanosomiasis and cryptosporidiosis prevention only on transmission



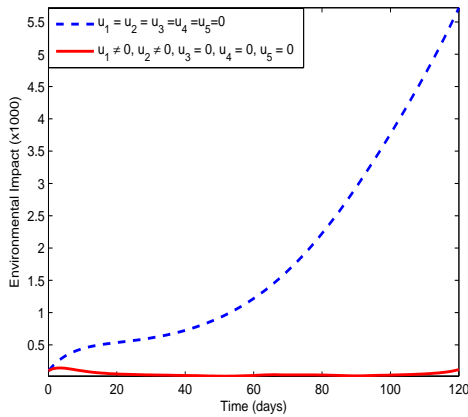
(a)

Fig. 28: Simulations of the trypanosomiasis-cryptosporidiosis model showing the effect of trypanosomiasis and cryptosporidiosis prevention only on transmission



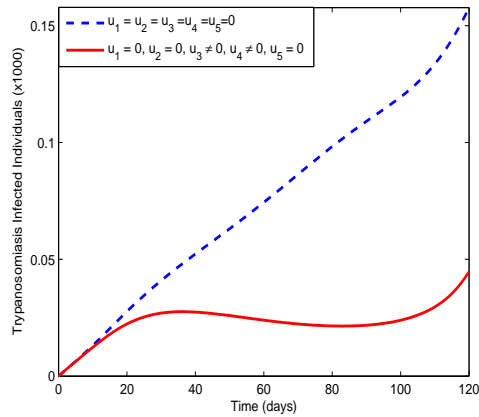
(a)

Fig. 30: Simulations of the trypanosomiasis-cryptosporidiosis model showing the effect of trypanosomiasis and cryptosporidiosis prevention only on transmission



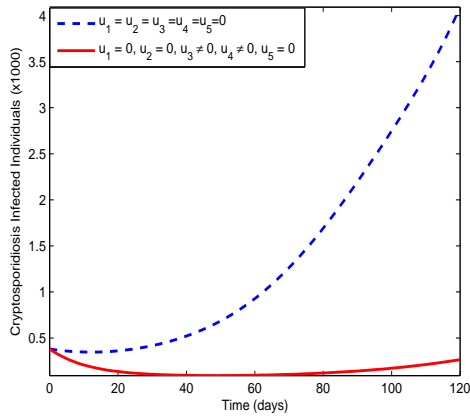
(a)

Fig. 29: Simulations of the trypanosomiasis-cryptosporidiosis model showing the effect of trypanosomiasis and cryptosporidiosis prevention only on transmission



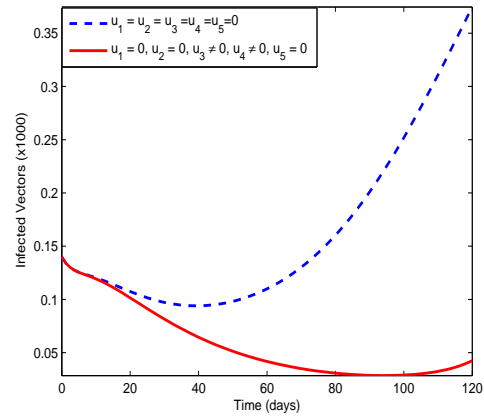
(a)

Fig. 31: Simulations of the trypanosomiasis-cryptosporidiosis model showing the effect of trypanosomiasis and cryptosporidiosis treatment only on transmission



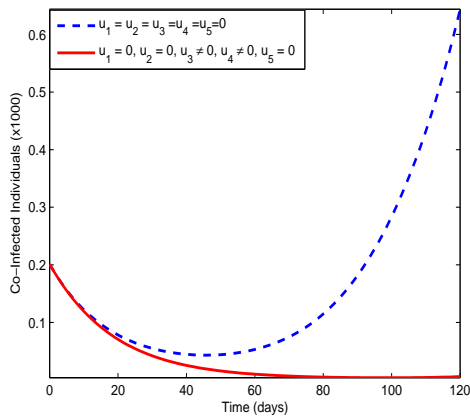
(a)

Fig. 32: Simulations of the trypanosomiasis-cryptosporidiosis model showing the effect of trypanosomiasis and cryptosporidiosis treatment only on transmission



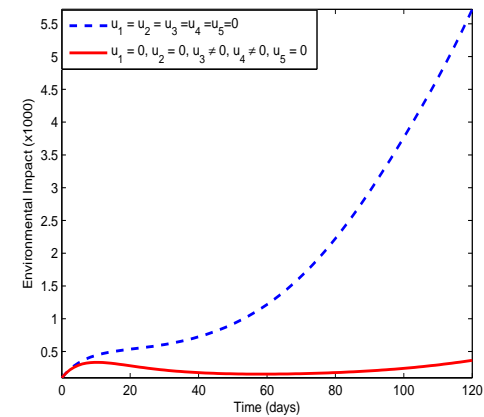
(a)

Fig. 34: Simulations of the trypanosomiasis-cryptosporidiosis model showing the effect of trypanosomiasis and cryptosporidiosis treatment only on transmission



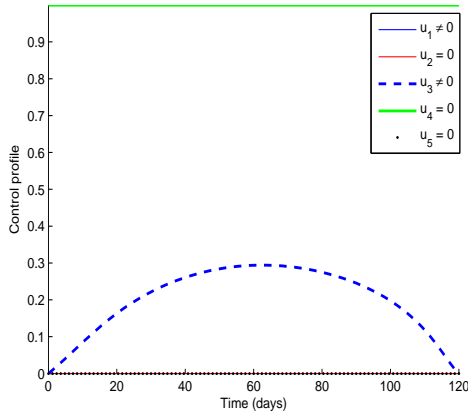
(a)

Fig. 33: Simulations of the trypanosomiasis-cryptosporidiosis model showing the effect of trypanosomiasis and cryptosporidiosis treatment only on transmission



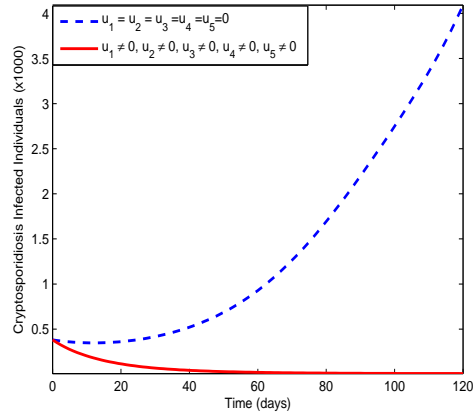
(a)

Fig. 35: Simulations of the trypanosomiasis-cryptosporidiosis model showing the effect of trypanosomiasis and cryptosporidiosis treatment only on transmission



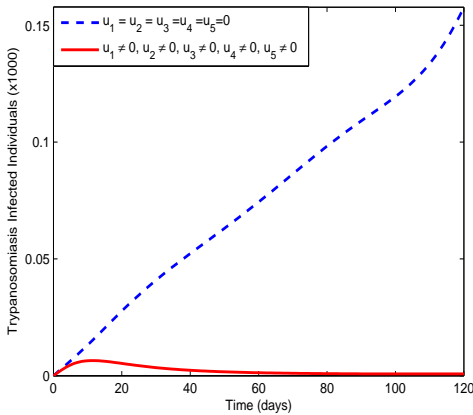
(a)

Fig. 36: Simulations of the trypanosomiasis-cryptosporidiosis model showing the effect of trypanosomiasis and cryptosporidiosis treatment only on transmission



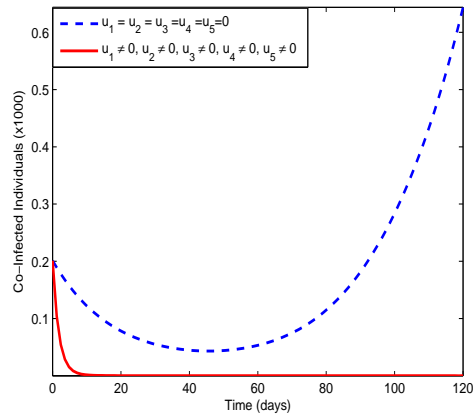
(a)

Fig. 38: Simulations of the trypanosomiasis-cryptosporidiosis model showing the effect of trypanosomiasis and cryptosporidiosis prevention with treatments on transmission



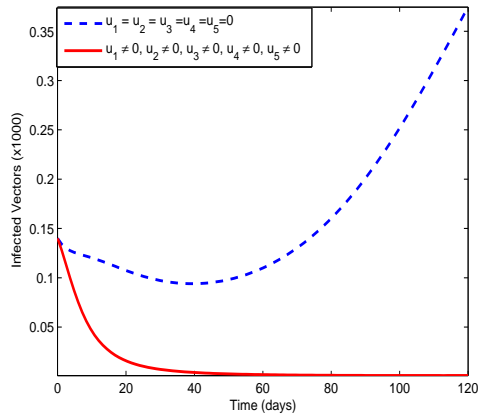
(a)

Fig. 37: Simulations of the trypanosomiasis-cryptosporidiosis model showing the effect of trypanosomiasis and cryptosporidiosis prevention with treatments on transmission



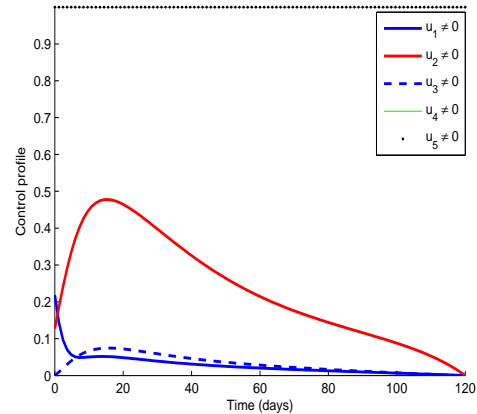
(a)

Fig. 39: Simulations of the trypanosomiasis-cryptosporidiosis model showing the effect of trypanosomiasis and cryptosporidiosis prevention with treatments on transmission



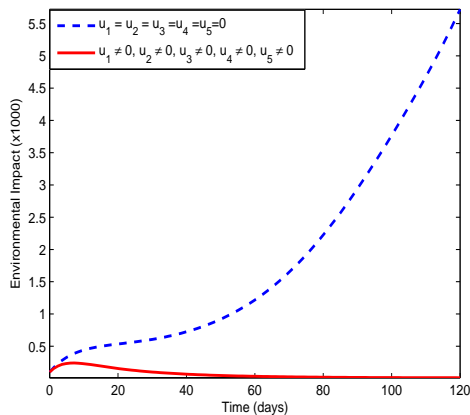
(a)

Fig. 40: Simulations of the trypanosomiasis-cryptosporidiosis model showing the effect of trypanosomiasis and cryptosporidiosis prevention with treatments on transmission



(a)

Fig. 42: Simulations of the trypanosomiasis-cryptosporidiosis model showing the effect of trypanosomiasis and cryptosporidiosis prevention with treatments on transmission



(a)

Fig. 41: Simulations of the trypanosomiasis-cryptosporidiosis model showing the effect of trypanosomiasis and cryptosporidiosis prevention with treatments on transmission

References

- [1] F.B. Augusto, M. Teboh-Ewungkem, A.B. Gumel, Mathematical assessment of the effect of traditional beliefs and customs on the transmission dynamics of the 2014 ebola outbreaks. *BMB Medicine*. **13(1)**, 1-17 (2015)
- [2] B. Bett, J. Hargrove, T.F. Randolph, R. Saini, A. Hassanali, J.M. Ndung'u, J.J. McDermott, Modelling the impact of tsetse-repellent on the transmission of cattle trypanosomiasis by *Glossina pallidipes* at Nguruman, Kenya. *Proceedings of the 10th International Symposium on Veterinary Epidemiology and Economics*. (2003)
- [3] C. Castillo-Chavez, B. Song, Dynamical model of tuberculosis and their applications. *Math. Biosci. Eng.* **1**, 361-404 (2004)
- [4] W.H. Fleming, R.W. Rishel, *Deterministic and stochastic optimal control*. Springer Verlag, New York (1975).
- [5] H.W. Hethcote, The mathematics of infectious diseases. *SIAM Review*. **42**, 599 - 653 (2000)
- [6] J.W. Hargrove, R. Ouifki, D. Kajunguri, G.A. Vale, S.J. Torr, Modeling the Control of Trypanosomiasis Using Trypanocides or Insecticide-Treated Livestock. *PLoS Neglected Tropical Diseases*. **6**, 5, e1615 (2012)
- [7] J.W. Hargrove, Tsetse population dynamics. In: Maudlin I, Holmes PH, Miles MA, eds. *The Trypanosomiasis*. Wallingford: CABI. 113-137 (2004)
- [8] J.W. Hargrove, R. Ouifki, J. Ameh, A general model for mortality in adult tsetse (*Glossina* spp.). *Medical and Veterinary Entomology*. **25**: 10 (2011)
- [9] J.B. Hugh, J.B.V. Marc, A dynamic population model for tsetse (Diptera: Glossinidae) area-wide integrated pest management
- [10] M.D. John Snow, *On the mode of communication of cholera*. John Churchill, New Burlington Street, England. (1855)

- [11] V. Lakshmikantham, S. Leela, A.A. Martynyuk, Stability Analysis of Nonlinear Systems. Marcel Dekker, Inc., New York and Basel. (1989)
- [12] J.P. LaSalle, The Stability of Dynamical Systems, Regional Conference Series in Applied Mathematics. SIAM, Philadelphia, Pa, USA, (1976).
- [13] A. Marc, G. Jean-Paul, A MODEL OF SLEEPING SICKNESS: OPEN VECTOR POPULATIONS AND RATES OF EXTINCTION. Analyse Non Linhaire et Modklisation.
- [14] J.J. McDermott, P. Coleman, Research into trypanosomosis epidemiology- the essential contribution of theory, models, diagnostics and field studies. Integrated Control of Pathogenic Trypanosomes and their Vectors (ICPTV) Newsletter. **1**, 11-15 (1999)
- [15] Z. Mukandavire, A.B. Gumel, W. Garira, J.M. Tchuente, Mathematical analysis of a model for HIV-Malaria co-infection. Mathematical Biosciences and Engineering. **6**: 333 - 362 (2009)
- [16] S. Mushayabasa, C.P. Bhunu, Is HIV infection associated with an increased risk for cholera? Insights from mathematical model. Biosystems. **109**, 203-213 (2012)
- [17] S. Mushayabasa, C.P. Bhunu, Modeling Schistosomiasis and HIV/AIDS co-dynamics. Computational and Mathematical Methods in Medicine. **2011**, 15 pages, doi:10.1155/2011/846174 (2011)
- [18] S. Mushayabasa, C.P. Bhunu, N.A. Mhlanga, Modeling the Transmission Dynamics of Typhoid in Malaria Endemic Settings. Applications and Applied Mathematics: An International Journal. **9(1)**, 121-140 (2014)
- [19] E. Mtisi, H. Rwezaura, J.M. Tchuente, A mathematical analysis of malaria and Tuberculosis co-dynamics. Discrete and Continuous Dynamical Systems Series B. **12(4)**, 827 - 864 (2009)
- [20] R.L.M. Nielan, E. Schaefer, H. Gaff, K.R. Fister, S. Lenhart, Modeling optimal intervention strategies for cholera. Bulletin of Mathematical Biology. **72**, 2004 -2018 (2010)
- [21] F. Nyabadza, B.T. Bekele, M.A. Rua, D.M. Malonza, N. Chiduku, M. Kgosimore, The implications of HIV treatment on the HIV-malaria coinfection dynamics: A modeling perspective. BioMed Research International. 2015, 14 pages (2015)
- [22] K.O. Okosun, O.D. Makinde, A co-infection model of malaria and cholera diseases with optimal control. Mathematical Biosciences. **258**, 19 - 32 (2014)
- [23] K.O. Okosun, O.D. Makinde, Optimal control analysis of hepatitis C virus with acute and chronic stages in the presence of treatment and infected immigrants. International Journal of Biomathematics. **7(2)**, 1450019 23 pages (2014)
- [24] M.W. Riggs, Recent advances in cryptosporidiosis: the immune response. Microbes and Infection, **4**, 1067-1080 (2002)
- [25] D.J. Rogers, A general model for the African trypanosomiasis. Parasitology. **97**: 193-212 (1988)
- [26] M.A. Safi, S.M. Garba, Global stability analysis of SEIR model with Holling Type II incidence function. Computational and Mathematical Methods in Medicine. **1** - 8 (2012)
- [27] S. Yeong., Modelling tsetse fly host preference and African trypanosomiasis in Cameroon park. MSc Thesis, Ohio State University. (2001)
- [28] The Merck veterinary manual for veterinary professionals. http://www.merckmanuals.com/vet/circulatory_system/blood_parasites/trypanosomiasis.
- [29] R.C.A. Thompson, A.J. Lymbery, A. Smith, Parasites, emerging disease and wildlife conservation. International Journal for Parasitology. **40**, 1163-1170 (2010)
- [30] S.J. Torr, G.A. Vale, Is the Even Distribution of Insecticide-Treated Cattle Essential for Tsetse Control? Modelling the Impact of Baits in Heterogeneous Environments. PLoS Negl Trop Dis. **5**, e1360 (2011)
- [31] P. Van den Driessche, J. Watmough, Reproduction numbers and sub-threshold endemic equilibria for compartmental models of disease transmission. Math. Biosci. **180**, 29 - 48 (2002)
- [32] Z. Weike, Global dynamics and applications of an epidemiological model for hepatitis C virus transmission. Discrete Dynamics in Nature and Society. **1**, 1 - 13 (2015)
- [33] Z. Zhang, T.A. Kwembe, Qualitative analysis of a mathematical model for malaria transmission and its variation. Tenth MSU Conference on Differential Equations and Computation Simulations. Electronic Journal of Differential Equations, Conference 23. 195 - 210 (2016)



Kazeem Oare Okosun is presently in the Department of Mathematics, Vaal University of Technology, Vanderbijlpark, South Africa. He graduated from the Faculty of sciences, Federal University of Technology Akure Nigeria in 2003. He received his Ph. D degree on Applied Mathematics, University of the Western Cape, South Africa in 2010. His research interests are mainly: Biomathematics, Scientific and Mathematical Computations, Mathematical Modelling.



Mirirai Mukamuri received an MSc (Master of Science) in Applied Mathematics specializing in Operations Research from the National University of Science and Technology, Zimbabwe. Currently, pursuing his PhD in Operations Research with University of South Africa. His current research interests include: Stochastic semi-infinite programming, Simulation Modelling and Mathematical modelling of epidemiological systems.

**Oluwole Daniel**

Makinde is presently a Distinguished Professor of Computational and Applied Mathematics at the Faculty of Military Science, Stellenbosch University, South Africa. He is also an Adjunct Professor at the NM-AIST in

Arusha-Tanzania; visiting Professor at PAUISTI in Nairobi-Kenya, visiting Professor at AUST in Abuja-Nigeria. He was a Senior Professor & Director of Postgraduate Studies and the founding Director of Institute for Advanced Research in Mathematical Modelling and Computations at CPUT- South Africa (2008-2013), Professor and Head of Applied Mathematics at University of Limpopo in South Africa (1998-2008). His main research interests are: Mathematical Modelling, Bio-Mathematics, Computational Mathematics, Fluid Mechanics, Nanofluid Dynamics, Heat and Mass Transfer and Hydrodynamic Stability. He is a Fellow of African Academy of Sciences, Fellow of Papua New Guinea Mathematical Society and Secretary General of African Mathematical Union. He won several prestigious academic research awards including: African Union Kwame Nkrumah Continental Scientific Award; South African NRF/ NSTF- TW Kambule Senior Researcher Award and Nigerian National Honour Award - Member of Order of the Federal Republic (MFR). He is a reviewer, editor and editorial board member of several international journals in the frame of Engineering Science, Applied Mathematics and Computations.